CORAL RECORDS OF RADIOCARBON VARIABILITY IN THE CENTRAL TROPICAL PACIFIC DURING THE LAST MILLENNIUM

A Thesis
Presented to
The Academic Faculty

by

Laura K. Zaunbrecher

In Partial Fulfillment
Of the Requirements for the Degree
Master in Science in the
School of Earth and Atmospheric Sciences

Georgia Institute of Technology
May 2009

Coral Records of Radiocarbon Variability in the Central Tropical Pacific During the Last Millennium

Approved by:

Dr. Kim Cobb, Advisor
School of Earth and Atmospheric Sciences
Georgia Institute of Technology

Dr. Jean Lynch-Stieglitz
School of Earth and Atmospheric Sciences
Georgia Institute of Technology

Dr. Annalisa Bracco
School of Earth and Atmospheric Sciences
Georgia Institute of Technology

Dr. Yuhang Wang
School of Earth and Atmospheric Sciences
Georgia Institute of Technology

Dr. Ellery Ingall
School of Earth and Atmospheric Sciences
Georgia Institute of Technology

Date Approved: April 3, 2009

ACKNOWLEDGMENTS

I would like to acknowledge and extend my gratitude to the Georgia Institute of Technology and the people here who have made this thesis possible. First, the head of the Earth and Atmospheric Sciences department, Judy Curry, who saw my potential and offered the original research assistantship, without which, would have made graduate school impossible. Also, I thank the EAS faculty who fostered my love of earth science. And of course all my committee members for taking the time to read this.

In particular, I wish to thank Kim Cobb, my adviser and friend, who first introduced me to the world of paleoceanography. She demonstrates daily what it takes to be an effective scientist and is an inspiring role model. Her brilliance in science and elegance in writing continue to astonish me. I could not have asked for a better adviser.

I'm also grateful for the opportunity to work with the people in the KCCAMS lab at the University of California, Irvine, where I conducted the radiocarbon measurements used in this study. The co-PI of this project, Ellen Druffel, has also been a great mentor to me. Our countless discussions of ocean dynamics and coral biology have truly enlightened me in this field. Working with someone of Ellen's caliber is a rare gift. Also, I'm forever indebted to Sheila Griffin, who trained me in the carbonate lab; she is a tremendous asset to this project. In the radiocarbon prep lab, Gauciara Santos and John Southon provided able assistance when the vacuum line was leaking or when I broke the drill bit (again)!

Thank you so much to everyone who helped with the interpretation of this data, especially Robbie Toggweiler, Keith Rodgers, and Warren Beck. Much thanks to Warren Beck for quickly making room for me at the University of Arizona ^{14}C preparation laboratory, the swiftness of supplying me with results, and all those cups of coffee. This wouldn't have been possible without the assistance of Richard Fairbanks and Rick Mortlock for providing the modern Christmas coral used in this study. I also wish to thank Mike Evans for providing the Christmas coral $\delta^{18}O$ and $\delta^{13}C$ datasets.

Thanks to Todd Walters, Yolande Berta, and Charlie Cappozi of the Georgia Tech Materials Science and Engineering department, for the SEM and sputter-coating training.

Much thanks also to Dr. W. Crawford Elliott of Georgia State University for the quick and efficient assistance in providing XRD training and results.

Of course all the people in my lab who made our lab a wonderful working environment. Nitya Sharma, not only a lab tech but a confidant, a true friend. Hussein Sayani, your assistance and enthusiasm while working on the diagenesis portion of this project made those long hours at the SEM fly by. Julien Emile-Geay, Intan Suci Nurhati, and James Herrin, for all the help you have provided me, and of course, assistance in tracking down our advisor when we need her!

There are certain professors that I would not be here without. John Meriwether, my undergraduate physics advisor who introduced me to world of radioactive isotopes. It was Dr. Meriwether, along with Tommy Michot, who took me on my first field

expedition to the hot, muggy, misquito-riden, wetland, Catahoula Lake. I never knew how fun it could be to go out into a swamp on an airboat to collect mud!

Most importantly, I need to thank my large family for their encouragement and support. In particular, my brothers: Nick, for the wisdom only an older brother can provide; Matt, for your competitive nature, which will always be a inspiration to me; Benjamin, for your ability to triumph when others doubt you, your strength and maturity beyond your years, and your God-given brilliance. Thank you all for the healthy dose rivalry and competition in 'Chaos Manor' but mostly the love and support for one another. Analise, my best friend, my twin sister, my other half. We did it. Here we are finishing our graduate education together, like we dreamed of as little girls.

My parents played a crucial role in getting me to where I am today; their encouragement for my love of science and mathematics, and most of all, believing in me. Mom and Dad, thank you for my intellectually stimulating upbringing.

Austin Cramer**,** my love and my rock. You have been here for me every hard step of the way to finally reaching this accomplishment. I know you've had a taste for grad school with me, all the background templates you designed for my presentations, spicing up all my photos. What would I do without you? Without your faith and support I may not have made it through those all-nighters and painfully stressful deadlines.

And of course my absolute best friends, Brie Moore, Rachel White, Jeanne Menard Elfert, Krissa Soisson Stiger, and Kristin Troxclair. Thank you.

TABLE OF CONTENTS

LIST OF TABLES

LIST OF FIGURES

SUMMARY

Ocean circulation changes in the tropical Pacific strongly influence global climate, as demonstrated during El Niño-Southern Oscillation (ENSO) extremes. Understanding the causes of past variability in tropical Pacific circulation and their relationship to climate change will help to predict how future climate may evolve under anthropogenic radiative forcing. I measure fossil coral radiocarbon ($\Delta^{14}C$) from Palmyra (6°N, 162°W) and Christmas (2°N, 157°W) Islands in the central tropical Pacific to reconstruct high-resolution records of tropical Pacific ocean circulation variability over the last millennium. Variations in coral $\Delta^{14}C$ from Palmyra and Christmas reflect a combination of the atmospheric concentration of ^{14}C at the time of growth, $\Delta^{14}C$-depleted waters associated with equatorial upwelling, and $\Delta^{14}C$ -enriched waters advected from the western tropical Pacific. Existing oxygen isotopic ($\delta^{18}O$) records of the Palmyra and Christmas fossil corals reveal a rich history of interannual to centennial variability in sea-surface temperature (SST) and salinity over the last millennium [*Cobb et al*., 2003b]. My approach targets specific time intervals associated with strong interannual to centennial-scale coral $\delta^{18}O$ anomalies for high-resolution $\Delta^{14}C$ analysis. Seasonally-resolved $\Delta^{14}C$ measurements are used to compare interannual $\Delta^{14}C$ variability across the 10^{th}, 13^{th}, 15^{th}, 17^{th}, and 20^{th} centuries. Annually-resolved $\Delta^{14}C$ measurements are used to compare decadal to centennial-scale $\Delta^{14}C$ variations from the 10^{th}, 12^{th} - 15^{th} and 17^{th} centuries. SEM photos are used to assess the fidelity of the coral $\Delta^{14}C$ records with respect to post-depositional alteration of the coral skeleton. I find evidence for minor dissolution and addition of secondary aragonite, but my results indicate that coral $\Delta^{14}C$ is only

compromised after moderate to severe diagenesis. Despite strong ENSO signals in modern and fossil coral $\delta^{18}O$, our data show no statistically significant interannual variability in coral ^{14}C. There is a centennial-scale increase in coral radiocarbon from the Medieval Climate Anomaly (MCA, ~900-1200AD) to the Little Ice Age (LIA, ~1500-1800). I use a box model of central tropical Pacific $\Delta^{14}C$ contributions to show that this centennial-scale trend over the last millennium is largely explained by centennial-scale changes in atmospheric ^{14}C. However, large 12th century depletions in Palmyra coral $\Delta^{14}C$ data cannot be explained by atmospheric ^{14}C variability and likely reflect a roughly two-fold increase in upwelling and/or a significant change in the ^{14}C of higher-latitude source waters reaching the equatorial Pacific during this time. Conversely, significantly enriched Christmas coral $\Delta^{14}C$ values during the 16th century are consistent with a two-fold reduction in upwelling strength and/or the advection of high-^{14}C waters to the equatorial thermocline from higher latitudes.

1. INTRODUCTION

Ocean circulation changes in the tropical Pacific strongly influence global climate, as demonstrated during El Niño-Southern Oscillation (ENSO) extremes. Normally, strong easterly trade winds in the tropical Pacific drive the upwelling of cold, deep water in the eastern to central tropical Pacific and push warm water into the Western Pacific Warm Pool (WPWP). The Southern Equatorial Current (SEC) is a westward-flowing surface current that mixes with upwelled waters along the equator. The Northern Equatorial Counter Current (NECC) flows from west to east just north of the equator, bringing Warm Pool waters in contact with upwelled waters in the central tropical Pacific. During strong El Niño events, a relaxation of the trade winds results in a large reduction in upwelling accompanied by an intensification of the NECC and a weaker SEC [*Taft and Kessler*, 1991]. This reorganization of equatorial currents reshapes SST patterns across the tropical Pacific basin, ultimately driving a reorganization of the large-scale atmospheric circulation. It also has profound consequences for the global carbon budget, as reduced upwelling does not allow for effective exchange between CO_2-rich deep waters and the atmosphere [*Takahashi*, 2004].

Instrumental data resolve seasonal to interannual variability in tropical Pacific circulation [*Picaut and Tournier*, 1991; *Donguy and Meyers*, 1996], but the relative magnitudes of decadal to centennial-scale changes in circulation remain unknown. Resolving such low-frequency variability and its relationship to low-frequency regional and global climate changes is critical to the improvement of ocean models used for climate prediction. Currently, coupled atmosphere-ocean climate models predict a wide

range of scenarios for 21st century tropical Pacific climate, ranging from "La Nina-like" (increased upwelling) to "El Niño-like" (reduced upwelling) [IPCC AR4, 2007]. By using paleo-reconstructions of tropical Pacific circulation and climate change over the last millennium, we can investigate the relationship between low-frequency circulation variability, climate change, and climatic forcing.

In this thesis, I present radiocarbon ($\Delta^{14}C$) records from modern and fossil corals from Palmyra (6°N, 162°W) and Christmas (2°N, 157°W) Islands to investigate changes in central tropical Pacific circulation over the last millennium. I assess the fidelity of the coral $\Delta^{14}C$ records with respect to subtle diagenesis using Scanning Electron Microscope (SEM) photos of the modern and fossil corals. The new coral ^{14}C records resolve the character of interannual, decadal, and centennial scale circulation variability from the Medieval Climate Anomaly (MCA; ~900-1200AD) through the Little Ice Age (LIA; ~1500-1800) to the 20th century. I compare the coral $\Delta^{14}C$ records to coral oxygen isotopic ($\delta^{18}O$)-based SST proxy records from the same corals to probe the relationship between circulation and surface climate variability on interannual to centennial timescales. I use a box model of central tropical Pacific seawater radiocarbon to constrain the relative influences of atmospheric ^{14}C variations versus changes in ocean circulation on coral $\Delta^{14}C$ variations during the last millennium. Lastly, I use SEM photos to characterize the potential contribution of diagenetic processes to the fossil coral ^{14}C records.

1.1 Radiocarbon as a Tracer for Water Mass Circulation

Spatial variations in seawater ^{14}C concentrations arise from horizontal and vertical mixing, where surface waters are relatively ^{14}C-enriched and deep waters are depleted. ^{14}C is a radiogenic isotope produced naturally in the atmosphere when cosmic rays interact with molecular nitrogen in the stratosphere. The ^{14}C atoms are quickly oxidized into $^{14}CO_2$, and then incorporated into the ocean though air-sea gas exchange. ^{14}C is a useful tracer of water mass mixing, as deep waters that have been isolated from the atmosphere for centuries to millennia are depleted in ^{14}C due to radioactive decay ($t_{1/2}$ = 5730 year), whereas surface waters are comparatively enriched. Large ^{14}C gradients are also present across the ocean surface [*Key et al.,* 2002] as upwelling brings relatively depleted ^{14}C waters to the ocean surface whereas air-sea gas exchange in the mid-ocean gyres drives ^{14}C enrichment in these areas. Thus, regional water masses are 'tagged' with a distinct ^{14}C signature depending on the regional oceanographic setting. Changes to regional seawater ^{14}C values though time imply changes in either horizontal or vertical mixing. For example, El Niño events result in a reduction of upwelling in the central and eastern tropical Pacific and a strengthening of easterly-flowing currents originating in the WPWP, profoundly reshaping the ^{14}C distribution of tropical Pacific surface waters [*Druffel,* 1981; *Brown,* 1993; *Rodgers,* 1997].

There have been two extensive surveys of surface and deep water radiocarbon concentrations over the past three decades. GEOSECS (Geochemical Ocean Sections Study, 1972-1979) [*Ostland and Stuiver,* 1980] and WOCE (World Ocean Circulation Experiment, 1990-2002) [*Key et al*., 1996; 2002] have provided snapshots of surface

water radiocarbon gradients, as well as surface to deep gradients. Both of these surveys took place well after extensive nuclear bomb testing in the 1950's caused a two-fold increase in atmospheric ^{14}C concentrations [*Nydal and Loveseth,* 1983], erasing so-called natural "pre-bomb" seawater ^{14}C gradients. Indeed, these datasets resolve large surface gradients in radiocarbon from ^{14}C-depleted upwelling regions to ^{14}C-enriched regions of subtropical gyres. These spatially-rich snapshots, while useful for mapping spatial ^{14}C gradients during the 1970's and 1990's, cannot be used to constrain the temporal variability of seawater ^{14}C concentrations through time.

1.2 Coral radiocarbon records

Corals have proven exceptional tools for the reconstruction of seawater radiocarbon concentrations as they incorporate the ^{14}C of the dissolved inorganic carbon of the seawater in which they grow, and can live for decades to centuries [*Druffel and Linick,* 1978; *Dunbar and Cole,* 1999*; Druffel et al.,* 2007]. Therefore, coral ^{14}C can be used to reconstruct seawater ^{14}C both long before the "bomb spike" [*Druffel*, 1981], and after the bomb spike [*Druffel,* 1987; *Druffel and Griffin*, 1993; *Guilderson and Schrag*, 1998; *Druffel et al*., 2001; *Grumet et at.,* 2004; *Grottoli*, 2007] at monthly resolution. Annual band counting in modern corals and/or U/Th dating in fossil corals ensure accurate, ^{14}C-independent absolute chronologies for the construction of coral-based records of seawater radiocarbon variability through time.

1.2.1. Coral ^{14}C records of the Suess Effect and Bomb Radiocarbon

The burning of ^{14}C-depleted fossil-fuels has caused a steady decline in twentieth century atmospheric ^{14}C levels, referred to as the "Suess Effect" [*Suess,* 1953]. Tree ring ^{14}C histories indicate atmospheric $\Delta^{14}C$ decreased by 20‰ from the late 1800s to 1955 [*Stuiver and Quay,* 1981]. The decrease in surface ocean ^{14}C was half that of the atmosphere (~10‰) [*Oeschger et al*., 1975] due to slow air-sea equilibration times and ocean mixing [*Oeschger et al*., 1975]. Coral ^{14}C records have captured the Suess Effect on the Great Barrier Reef, Australia and in surface waters off Hawaii [*Druffel and Griffin*, 1993, 1999; *Druffel et al*., 2001].

A profound reshaping of natural ^{14}C distributions occurred in conjunction with weapons testing during the 1950's and 60's [*Nydal and Loveseth,* 1983]. The steady incorporation the so-called "bomb ^{14}C" into the surface ocean was recorded by corals across the tropics, with upwelling sites being the last to record elevated ^{14}C values. The ^{14}C bomb pulse increased the surface-to-deep water ^{14}C gradient, such that upwelling events became more pronounced in coral ^{14}C records across the tropical Pacific [*Nozaki et al*, 1978; *Druffel*, 1987; *Druffel and Griffin*, 1993;, *Druffel*, 1997; *Guilderson and Schrag*, 1998; *Grotolli*, 2003; *Grumet et al.*, 2004]. Today, the vast majority of coral ^{14}C records cover only the post-bomb interval, and there is relatively little information on "pre-bomb" marine ^{14}C spatial or temporal variability.

1.2.2. Coral ^{14}C records of the El Niño Southern Oscillation

Tropical Pacific coral ^{14}C records also resolve upwelling variability associated with ENSO, recording depleted values during La Niña events and enriched values during El Niño events [*Druffel*, 1981; *Brown*, 1993; *Guilderson and Schrag*, 1998]. Indeed, Guilderson et al., [2004] used a mixed layer model equipped with radiocarbon to investigate interannual changes in tropical Pacific circulation by reproducing coral ^{14}C data from the Galapagos, Raratonga, and the Solomon Sea. Previous research with ^{14}C-equipped ocean models confirmed that seawater ^{14}C changes at coral sites including Guam, Galapagos, Fanning, and Canton should be sensitive to ENSO-related changes in tropical Pacific circulation [*Rodgers et al*., 1997; 2004].

1.2.3. Coral ^{14}C records of the Pacific Decadal Oscillation

The Pacific Decadal Oscillation is a pattern of interdecadal variability in the Pacific that has been captured in coral ^{14}C records. Guilderson and Schrag [1998] applied high-resolution coral ^{14}C measurements to a Galapagos coral to argue for a deeper thermocline in the eastern tropical Pacific upwelling zone beginning in 1976. A large increase in Galapagos coral ^{14}C values during the boreal winter upwelling season began in 1976, coincident with the so-called 1976 climate "regime shift" from cool-to-warm tropical Pacific SSTs [*Miller et al*., 1994, *Graham*, 1994; *Hare and Mantua*, 2000]. Subsequently, Rodgers [2004] used a ^{14}C-equipped ocean model to link the 1976 climate

shift to a reduction in the amount of ^{14}C-depleted Sub Antarctic Mode Water (SAMW) entering the equatorial undercurrent (EUC).

1.2.4. Diagenesis Effects on Modern and Fossil Coral ^{14}C

Submarine and subaerial diagenesis may alter the coral skeletal geochemistry and therefore introduce artifacts into coral paleoclimate reconstructions [*Bar-Matthews et al.,* 1993; *Enmar et al*., 2000; *McGregor et al*., 2003]. Examples of post-depositional diagenesis include dissolution, recrystallization, and/or coating by secondary aragonite or calcite. ^{14}C is especially sensitive to diagenesis involving recrystallization or secondary carbonate precipitation, because the addition of relatively young carbonate material to the original skeleton will add large amounts of ^{14}C [*Burr et al*., 1992], obliterating the subtle ^{14}C changes associated with water mass mixing. Chui et al., [2005] propose a two-step screening procedure before ^{14}C dating a fossil coral sample, including X-ray diffraction (XRD) screening and an extended hydrogen peroxide cleaning (which removes young organic contaminants). However, this screening will not detect secondary aragonite addition, which has been observed in young modern corals as well as fossil corals [*Enmar et al*., 2003; *Allison*, 2007].

Most coral diagenesis studies have focused on the implications of diagenesis for coral oxygen isotopes ($\delta^{18}O$), a commonly-used coral SST proxy [*Castellaro et al.,* 1999; *Enmar et al.,* 2000; *Müller et al*., 2001]. Such studies show that diagenesis often leads to more enriched coral $\delta^{18}O$ compositions because inorganic calcite and aragonite precipitated from seawater is enriched in $\delta^{18}O$ with respect to the coral skeleton [*Enmar*

et al., 2000; *Müller et al*., 2001; *Hendy*, 2007]. Coral $\delta^{18}O$ is inversely correlated to SST, so the addition of enriched $\delta^{18}O$ to the coral skeleton results in coral $\delta^{18}O$-based SST reconstructions that are artificially cool [*McGregor et al.*, 2003; *Allison*, 2007].

Diagenesis of fresh coral skeleton can occur in a matter of decades, both via dissolution and/or the precipitation of secondary aragonite [*Enmar et al.*, 2000; *Hendy*, 2007]. It is important to note that dissolution has no documented effect on coral ^{14}C or $\delta^{18}O$, so the primary concern for this study is the recrystallization and/or precipitation of secondary aragonite and/or calcite. As the diagenetic history of the beached fossil corals used in this study is unknown, careful diagenetic screening is conducted to characterize the potential effects of diagenesis on the coral ^{14}C records.

1.3 Oceanographic Setting

Palmyra (6°N, 162°W) and Christmas (2°N, 157°W) Islands are part of the Line Islands chain in the middle of the tropical Pacific Ocean (Figure 1.1). Palmyra sits in the Northern Equatorial Counter Current (NECC) which brings warm, fresh waters eastward from the Western Pacific Warm Pool (WPWP). Located nearer to the equator than Palmyra, Christmas Island is bathed in the cool, salty waters of the westward flowing SEC, which carries the signature of equatorial wind-driven upwelling [*Reverdin*, 1994].

Currents in the central tropical Pacific vary in strength and location with seasonal to interannual changes in the tropical Pacific wind regime. Each year, the surface winds in the central equatorial Pacific change from northeasterly winds during boreal winter to southeasterly winds during boreal summer [*Reverdin*, 1994]. As a result, Palmyra

receives cool, salty water from the SEC through northward Ekman transport during boreal winter months but is dominated by NECC waters during boreal summer [*Wyrtki and Kilonsky*, 1984].

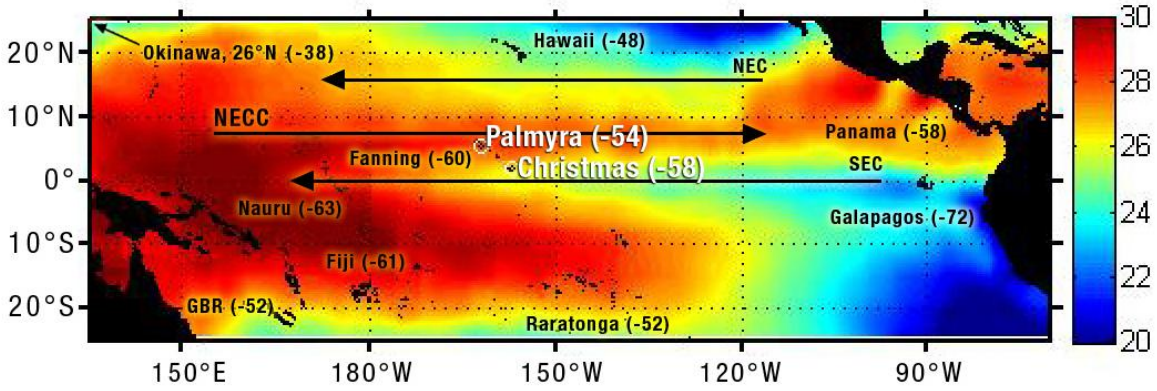

Figure 1.1 – Map of average Sea Surface Temperature in the Pacific [*Smith and Reynolds*, 2007] (*NOAA_ERSST_V3 data provided by the NOAA/OAR/ESRL PSD, Boulder, Colorado, USA, from their Web site at http://www.cdc.noaa.gov/)* **and average pre-bomb radiocarbon as measured in corals:** Galapagos [*Druffe*l, 1981], Rarotonga [*Guilderson et al, 2001*], Fiji [*Toggweiler et al, 1991*], Great Barrier Reef [*Druffel and Griffin, 1993*] Panama [Druffel, 1987], Fanning [*Druffel*, 1987], Nauru [*Guilderson et al, 1998*], Hawaii [*Druffel et al, 2001*], Okinawa [*Konishi et al, 1981*]. The major surface currents are represented by the long arrows.

The tropical Pacific is normally characterized by a zonal SST gradient defined by cold, upwelled waters in the eastern cold tongue and warm, stratified waters in the WPWP. In the atmosphere, strong easterlies prevail at the surface along the equator, with divergence and subsidence in the eastern cold tongue region and convergence and ascent over the WPWP. Strong coupling between the atmosphere and ocean means that during El Niño conditions, a reduction in the easterly trade winds results in weakened upwelling

and a reduced zonal SST gradient, which in turn weakens the trade winds. The reduction in trade winds and upwelling means that the NECC plays a stronger role in central tropical Pacific circulation, with a dramatically reduced or even nonexistent SEC. When an intensification of the trade winds and the zonal SST gradient occurs during La Niña conditions, upwelling intensifies and the SEC plays a dominant role in central tropical Pacific circulation.

Modern and fossil coral oxygen isotopic ($\delta^{18}O$) records from Palmyra Island have provided exceptional reconstructions of ENSO and low frequency climate variability in the central tropical Pacific during the last millennium [*Cobb et al*., 2001; 2003b]. The existing 20th century coral $\delta^{18}O$ records from Palmyra and Christmas islands are highly correlated to regional SST records (R =-0.65 and R=-0.84 with NIÑO3.4, respectively) [*Cobb et al.*, 2001; *Evans et al.*, 1999]. The Palmyra fossil coral $\delta^{18}O$ records reveal that during the MCA the tropical Pacific was likely cooler and/or drier than the pre-industrial period, with moderate ENSO activity. The LIA was characterized by more frequent and intense ENSO events, with average climate conditions similar to pre-industrial values. Generally speaking, the records reveal prominent low-frequency decadal-to-centennial scale changes in tropical Pacific climate.

By comparing the existing coral $\delta^{18}O$ records to newly generated coral ^{14}C records from Palmyra and Christmas, we can investigate the relationship between surface climate (SST and hydrology) and water mass circulation on interannual to centennial timescales. One would expect that periods of stronger upwelling would be recorded as more enriched $\delta^{18}O$ (signifying cooler, drier conditions) and more depleted ^{14}C (signifying the presence of deeper water at the surface). Conversely, periods of reduced

upwelling might be recorded as relatively depleted $\delta^{18}O$ (warmer, wetter conditions) and relatively enriched ^{14}C (isolation of deep waters from surface).

2. Methods

For the most part, the $\delta^{18}O$ records and chronological constraints for the modern and fossil corals analyzed in this study are previously published. The Palmyra modern coral $\delta^{18}O$ record was originally published by Cobb et al., [2001]. The Christmas modern coral (PP7-3) was originally published by Evans et al., [1999]. With the exception of Christmas fossil coral M-2 and Palmyra fossil corals A27 and SB3B, the relevant $\delta^{18}O$ records and U/Th dates for all the fossil corals are reported in Cobb et al., [2003a; 2003b].

2.1. Isotope Measurements

2.1.1 Coral $\delta^{18}O$ Measurements

Most of my ^{14}C sampling was conducted on the exact slab corresponding to the published coral $\delta^{18}O$ records, whose climate-related variability guided my ^{14}C sampling. However, in the case of the Palmyra modern coral and a 17th century Palmyra fossil coral (SB3), I generated new $\delta^{18}O$ profiles for duplicate cores which were then used for ^{14}C sampling. This was necessary because slab geometries prevented us from drilling the large, closely-spaced samples required for ^{14}C analysis. The duplicate coral $\delta^{18}O$ profiles were exactly matched to the original coral $\delta^{18}O$ profiles, allowing for the assignment of firm chronological constraints. Coral powders weighing 60 to 90μg were drilled every 1mm along the coral axis of maximum growth using a table mounted, low-speed Dremel

drill. The powders were analyzed for $\delta^{18}O$ on a GV Isoprime Mass Spectrometer at the Georgia Institute of Technology, with an external precision of ±0.05‰ (1σ; N=550). $\delta^{18}O$ is reported as per mil deviation from NBS-19 according to the formula:

$$\delta^{18}O\ ‰ = \left[\left(\frac{\left(\frac{^{18}O}{^{16}O}\right)_{Sample}}{\left(\frac{^{18}O}{^{16}O}\right)_{NBS-19}}\right) - 1\right] \times 1000\ (‰) \qquad (2.1)$$

2.1.2 Coral $\Delta^{14}C$ Measurement

As a result of the high cost of a single $\Delta^{14}C$ measurement, the coral $\delta^{18}O$ records were used to target specific time intervals for $\Delta^{14}C$ analysis. Large amplitude ENSO, decadal, and centennial $\delta^{18}O$ variations were targeted as the likeliest periods for major circulation changes and thus the largest $\Delta^{14}C$ signals.

A 1mm-wide diamond-tipped bit was used in a hand-held Dremel tool to drill 6-10mg of powder from coral slabs. Sub-annual $\Delta^{14}C$ samples were drilled every 1-3mm, corresponding to one sample every 1-2 months (~8 samples/year). Annual $\Delta^{14}C$ samples were drilled across an entire year of coral growth (10 to 25mm) guided by $\delta^{18}O$ chronologies and x-rays of the coral slabs. Coral $\Delta^{14}C$ samples were analyzed following established protocols outlined in Druffel et al., [2004]. Coral powders were prepared for analysis by acidification to CO_2 and conversion to graphite using an Fe catalyst and the hydrogen reduction method [*Vogel et al.*, 1984]. Coral ^{14}C was measured on the Keck

Carbon Cycle Accelerator Mass Spectrometer (KCCAMS) at the University of California, Irvine with a precision of ±1.8‰ (1σ, N=129) [*Southon*, 2004] based on over two years of measurements of a coral standard. Radiocarbon values are reported in per mil deviations from an oxalic acid standard (representing the activity of 19th century wood) as specified in Stuvier and Polach [1977], according to the following formula:

$$\Delta^{14}C\,‰ = \left[\left(\frac{\left(\frac{^{14}C}{^{12}C}\right)_{Sample}}{\left(\frac{^{14}C}{^{12}C}\right)_{Standard}}\right) - 1\right] \times 1000\,(‰) \qquad (2.2)$$

^{13}C was measured sequentially on the AMS, along with the ^{14}C and ^{12}C. The samples were corrected for fractionation using the measured δ^{13}C and normalized to a δ^{13}C = -25‰, according to the following equation:

$$\Delta^{14}C_{Corrected} = \Delta^{14}C_{Measured}\left(1 - \frac{2(25+\delta^{13}C)}{1000}\right)(‰). \qquad (2.3)$$

The Δ^{14}C values are subsequently age corrected to the year 1950 when Δ^{14}C = 0‰ (by definition) using published U/Th dates [*Cobb et al*. 2003a].

$$\Delta^{14}C_{Age-Corrected} = \Delta^{14}C_{Corrected}\exp[\lambda(-year + 1950)]\,(‰) \quad (2.4),$$

where $\lambda = 1/8267\ yr^{-1}$ is the decay rate constant based on the half-life of radiocarbon (5730 years). The age correction facilitates the comparison of coral ^{14}C of different ages and isolates the variability of radiocarbon in the water mass.

Numerous duplicates tested the reproducibility of the graphitization procedure and instrument performance. Of the first 48 samples, 9 were duplicated and they were found to be within 1σ of each other. For the rest of the study, one in ten samples was duplicated. Of the total 235 samples, there were 31 duplicate pairs, all within analytical error of each other. The analytical error for coral ^{14}C measurements at the UCI AMS is reported as ±1.8‰ (1σ, N=129), and is derived from repeat measurements of coral standards all made from the same coral powder.

To test the reproducibility of the UCI coral ^{14}C measurements, 30 samples from the Palmyra and Christmas corals were measured at the University of Arizona (UA) AMS facility. Sub-annual samples (1mm wide solid coral slivers) were cut using a band saw from the two modern corals and three fossil corals. Sampling locations were guided by $\delta^{18}O$ chronologies and the UCI coral $\Delta^{14}C$ results to target the largest potential ^{14}C variability. Coral $\Delta^{14}C$ samples were analyzed following established protocols outlined in Burr et al., [1992]. Coral slivers were prepared for analysis by acidification to CO_2 and conversion to graphite using an Fe catalyst and the zinc reduction method [*Slota et al.,* 1984; *Marzaioli et al*., 2008]. The UA AMS $\Delta^{14}C$ error is based on the counting and machine error, and the blank uncertainty according to:

$$\sigma_{total} = \sqrt{\left(\sigma_{ce}^2 + \sigma_{me}^2 + \sigma_{bu}^2 \right)} \qquad (2.5)$$

The total error for the University of Arizona coral ^{14}C measurements presented in this paper is ±4.0‰ (1σ, N>1000) [*Burr et al.*, 1998].

2.2 Diagenesis screening by SEM

A Hitachi S-800 field emission gun Scanning Electron Microscope (SEM) at the Georgia Tech Materials Science and Engineering department was used to investigate microscopic alterations to the coral skeletal morphology. Small pieces of the coral skeleton (<5mm on a side) were chipped off and mounted on SEM studs using double sided carbon tape. An Ernest Fullam SputterCoater was used to prepare the coral samples for the SEM by coating them with ~200Å of gold.

2.3 Mixed Layer Model

In order to understand the causes of ^{14}C variability in the surface waters at Palmyra on interannual to centennial timescales, I modified a mixed layer model presented in Druffel et al., [1997] to fit the specifics of the central tropical Pacific. The model makes very basic assumptions that attempt to distill the key dynamics of the central tropical Pacific circulation system into a simple box model that evolves seawater radiocarbon concentrations through time (Figure 2.1). The main sources of seawater radiocarbon variability are horizontal advection, vertical advection, and air-sea CO_2 exchange.

Horizontal advection contributes ~30% of the waters entering the Palmyra box, and its temporal evolution over the last millennium is assumed to follow the global mixed layer ^{14}C estimate of Hughen et al., [2004]. The Hughen et al. [2004] model uses the INTCAL04 [*Reimer et al.,* 2004] atmospheric calibration curve together with tree-ring ^{14}C proxy data, to reconstruct the global average sea surface radiocarbon concentration over the last millennium (hereafter referred to as Marine04). The horizontal advection component in the equatorial Pacific likely represents a combination of the Marine04 global average surface waters (higher ^{14}C, better equilibrated with atmosphere) and upwelled waters (lower ^{14}C, poorly equilibrated with atmosphere) that would damp the Marine04 ^{14}C variability. Therefore, our use of Marine04 as the horizontal advection contribution represents an upper limit on the contribution of atmospheric ^{14}C variations to surface water ^{14}C variations at Palmyra. Vertical advection originates from seven layers down to 200m deep, each decreasing in ^{14}C content. The choice of 200m as a maximum depth of upwelling is based on Fine et al., [1983], although some recent studies support a shallower source of upwelled waters ranging from 180m [*Bryden and Brady*, 1985] to 140m [*Wiesberg and Qiao,* 2000]. Seawater radiocarbon at 200m is set to -100‰ based on model data from Matsumoto and Key [2004].

The mixed layer depth is set to 80m, which represents an intermediate value between interannual extremes of ~200m and ~0m [*Johnson and McPhaden*, 2000]. W_1, the water mass renewal rate, is set to a constant value 0.24 yr^{-1}. This value comes from tuning the forward model (equation 2.5) to generate a steady state, prebomb $\Delta^{14}C$ value of -54‰ (the measured Palmyra modern coral pre-bomb value), an approach outlined in Druffel et al., [1989;1997]. The atmospheric ^{14}C concentration follows the INTCAL04

reconstruction [*Reimer et al.*, 2004]. Seawater radiocarbon values in the Palmyra box evolve according to the equation:

$$P(t+\Delta t) = P(t) + [M(t) - P(t)]\Delta t + [k_{-1}A(t) - k_1 P(t)]\Delta t + W_1(t) \times \sum S_i \times \Delta t \times [\sum D_i(t) - P(t)], \quad (2.6)$$

where P(t) is the radiocarbon concentration at Palmyra at time t, M(t) is the Marine04 global ocean radiocarbon values as modeled in Hughen et al., [2004], Δ(t) is the time step (set to 1 year in this case), k_{-1} represents the input rate of $^{14}CO_2$ from the air to the sea surface, and k_1 represents the rate constant of the output of $^{14}CO_2$ from the sea surface to the air, $W_1(t)$ is the water mass renewal rate, S_i is the mixing constant from the surface to deep boxes, and D_i is the water radiocarbon value in the deep boxes 1 through 7. The values for k_1 and k_{-1} are modeled after Druffel et al. [1997] and are dependent upon the atmospheric concentration of CO_2, mixed-layer depth, wind speed, total CO_2, and piston velocity, but are held constant in this model. I use a time step of one year and integrate the model for 1,500 years, from 650AD to 1950AD. Here, S_i = 1, 0.5, 0.4, 0.35, 0.3, 0.25, and 0.2, as deeper layers contribute progressively less volume to the surface box.

A reverse model calculates upwelling rates (W_1) based on inverting the equation above (equation 2.6) and plugging in Palmyra coral ^{14}C (equation 2.7).

$$W_1 = \frac{P(t+\Delta t) - P(t) - [M(t) - P(t)] - [k_{-1}A(t) - k_1 P(t)]}{[\sum D_i(t) - P(t)] \times \sum S_i} \quad (2.7)$$

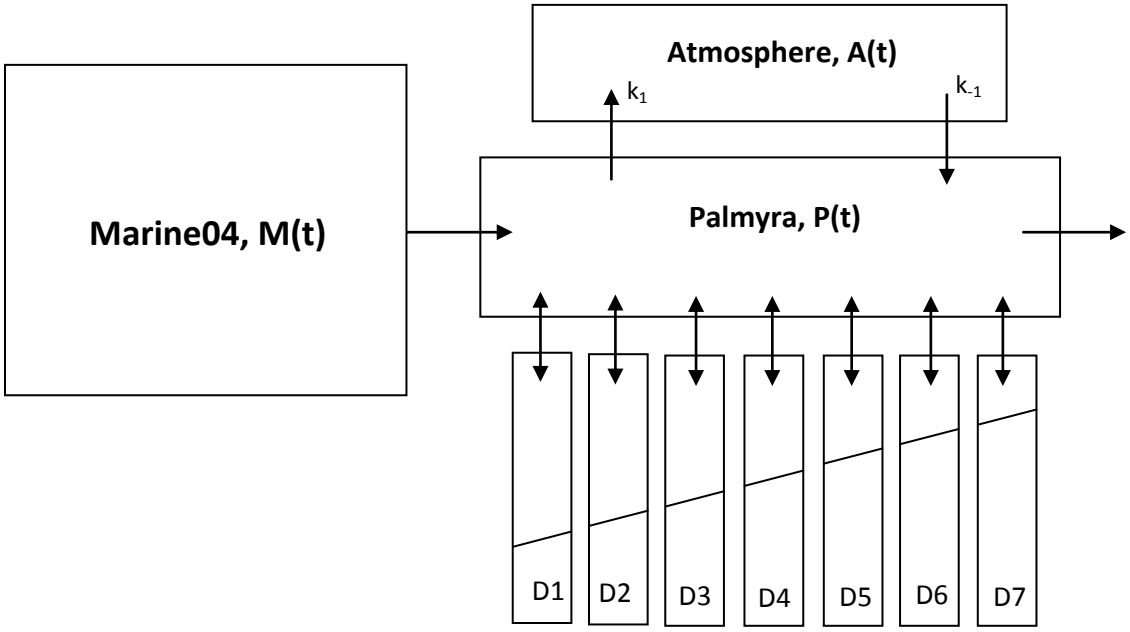

Figure 2.1: Schematic of the Mixed Layer Box Model. Modeled Marine04 values from the box M(t) are input into the Palmyra box, P(t) as the advective term. The atmospheric box, A(t), varies as INTCAL04 [*Reimer et al.,* 2004]. The seven deep layers in P(t) are held constant at $D_{i=1:7}$= -60‰, -65‰, -75‰, -85‰, -90‰, -95‰, -100‰ and mix to the surface in ratios according to S_i (see text).

3. RESULTS

3.1. Interannual ^{14}C variability

I find insignificant changes in coral $\Delta^{14}C$ across the large 1941-1943 El Niño/La Niña cycle in modern corals from both Palmyra and Christmas Islands (Figure 3.1). I measured ^{14}C across this ENSO cycle because it represents the only large pre-bomb ENSO cycle common to both the Palmyra and the Christmas modern coral cores. Although there are large interannual variations in the coral $\delta^{18}O$ data from both islands, which track warm and cool ENSO-related SST in this area, the coral $\Delta^{14}C$ values remain nearly constant, with Palmyra averaging -54.8 ±1.59‰ (N=24) and Christmas averaging -58.2 ±1.66‰ (N=24) (Figure 3.1). The statistically significant offset between ^{14}C values from Palmyra and Christmas reflects the fact that Christmas is closer to the equatorial source of ^{14}C-depleted upwelling waters.

High-resolution sampling across six additional ENSO cycles recorded in modern and fossil coral $\delta^{18}O$ data from Palmyra and Christmas revealed similarly low ^{14}C variability (Figure 3.2). ENSO anomalies in 1917AD, 1655AD, 1431-1433AD, 1421-1422AD, and 943-945AD were analyzed in Palmyra corals and an ENSO cycle in 1537-1538AD was analyzed in a Christmas fossil coral. The 16th century Christmas fossil coral $\delta^{18}O$ data and U/Th dates are presented in Cobb et al., in prep. Additional high-resolution ^{14}C samples from Palmyra and Christmas corals measured at University of Arizona corroborate the data from UCI (Figure 3.2).

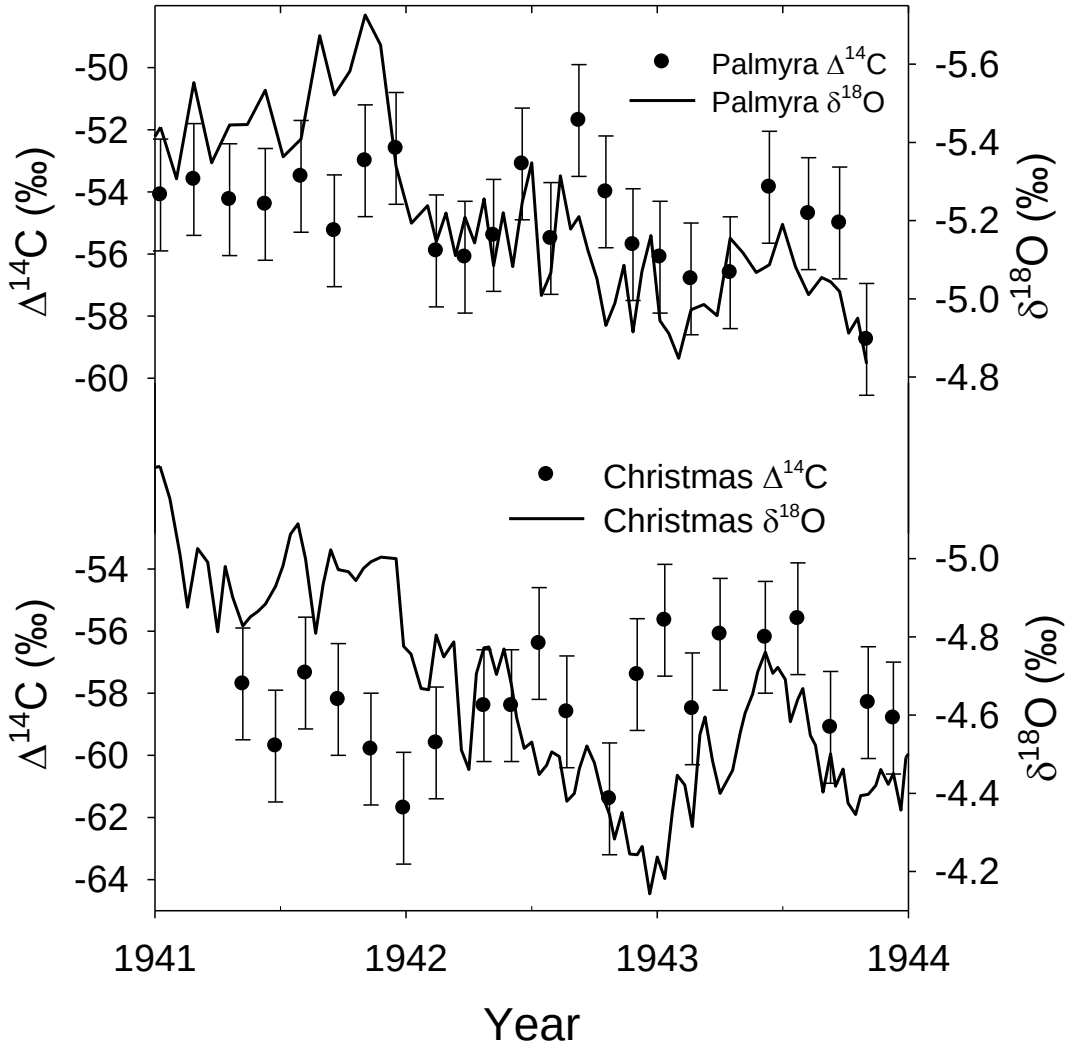

Figure 3.1: **Coral $\delta^{18}O$ and $\Delta^{14}C$ measured across the 1941-1943 ENSO cycle at Palmyra (top) and Christmas (bottom).** Error bars for coral radiocarbon reflect analytical uncertainties of ±1.8‰ (1σ).

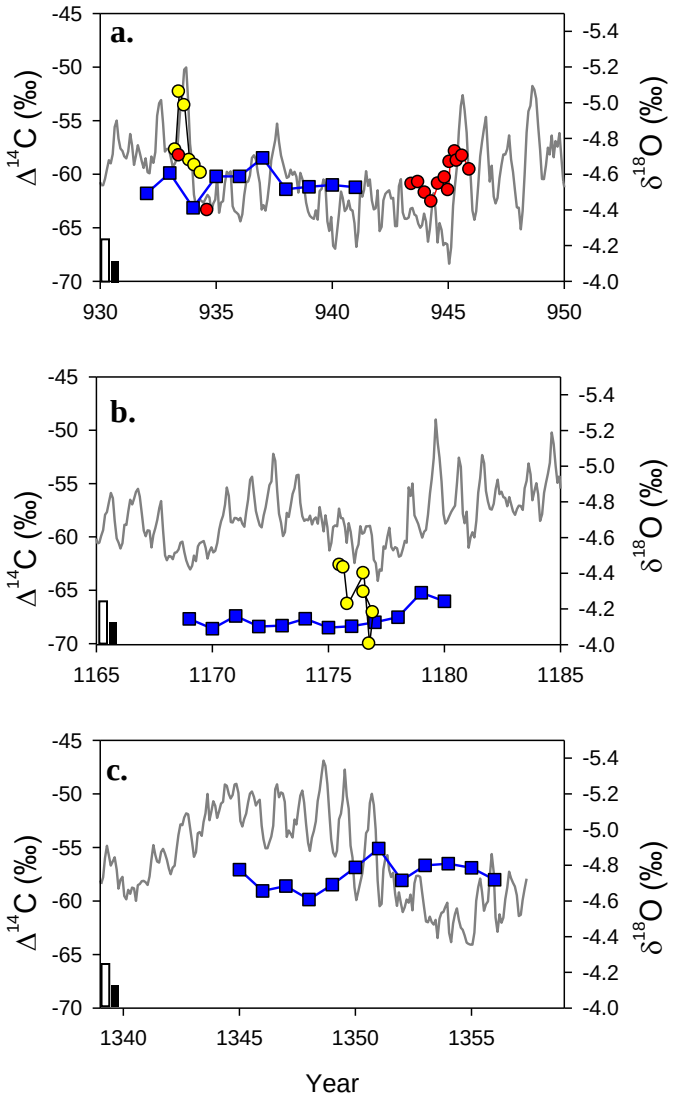

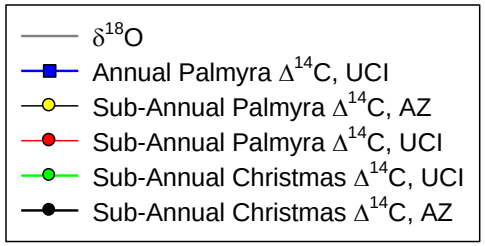

Figure 3.2: Comparison of all coral ^{14}C Measurements with coral $\delta^{18}O$. a.) 10th century Palmyra, NB12, **b.)** 12th century Palmyra, L17, **c.)** 14th century Palmyra, SB7, **d.)** 15th century Palmyra, SB5**, e.)** 16th century Christmas, M2, **f.)** 17th century Palmyra, SB3B, **g.)** Palmyra modern, **h.)** Christmas modern, PP7-3. The vertical thick black line represents the ±1.8‰ (1σ) standard error for UCI AMS, the vertical white rectangle represents the ±4.0‰ standard error at UA. $\delta^{18}O$ are from Cobb et al., [2003b]. (e) - Christmas Island $\delta^{18}O$ is presented in [*Cobb et al.*, in prep], the $\delta^{18}O$ axis has been shifted by 0.4‰, to account for greater $\delta^{18}O$ variability close to the equator, while the $\Delta^{14}C$ axis is shifted by +5‰ for the most enriched values of the record. (f) - The 17th century Palmyra box is extended by 5‰ on the $\Delta^{14}C$ axis and 0.2‰ on the $\delta^{18}O$ axis, to accommodate the enriched values during this time period. (h) - Christmas Modern coral $\delta^{18}O$ is from Evans et al., [1999]. All axes have equal scaling.

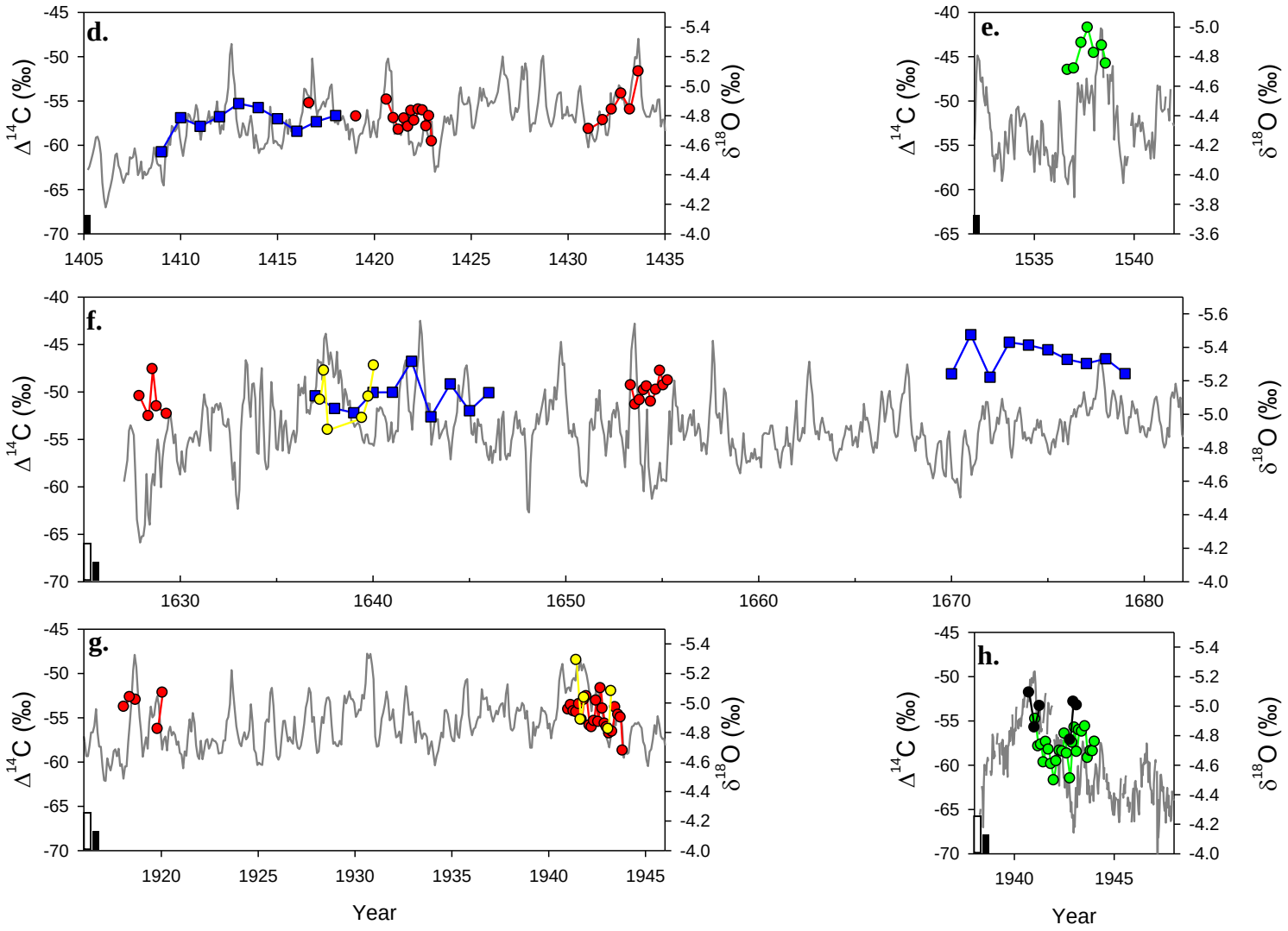

Figure 3.2: (Continued)

3.2 Decadal ^{14}C Variability

Large decadal-scale shifts in coral $\delta^{18}O$ were targeted for $\Delta^{14}C$ analysis to investigate lower frequency changes in surface ocean radiocarbon. Six fossil corals from Palmyra were sampled for annually-averaged $\Delta^{14}C$ variations during 932-941AD, 1169-1180AD, 1344-1356AD, 1409-1418AD, 1637-1647AD, and 1669-1680AD (Figure 3.3). The most pronounced feature in the 10th century coral $\delta^{18}O$ is a large decadal shift to heavier $\delta^{18}O$ values (warmer/wetter conditions) that occurs from 933 to 945AD. Radiocarbon exhibits a minimum of -63.4‰ in 934 and a maximum of -58.5‰ in 937, a statistically insignificant change (Figure 3.3a). The 12th century annual $\Delta^{14}C$ values are similarly constant, despite a large sub-decadal shift in $\delta^{18}O$ (Figure 3.3b). Coral $\Delta^{14}C$ samples from the 14th and 15th centuries range from -60.7‰ in 1409 to -55.3‰ in 1413, showing no significant decadal-scale variability (Figure 3.3c,d). The mid-17th century ^{14}C values vary from -52.6‰ in 1643 to -46.8‰ in 1642, a 5.8‰ range that is well within the 2σ uncertainty (±3.6‰) (Figure 3.3e). The late-17th century $\Delta^{14}C$ values are relatively constant (Figure 3.3f). We conclude that seawater ^{14}C at Palmyra did not vary across the large decadal-scale climate anomalies inferred from coral $\delta^{18}O$ during the last millennium.

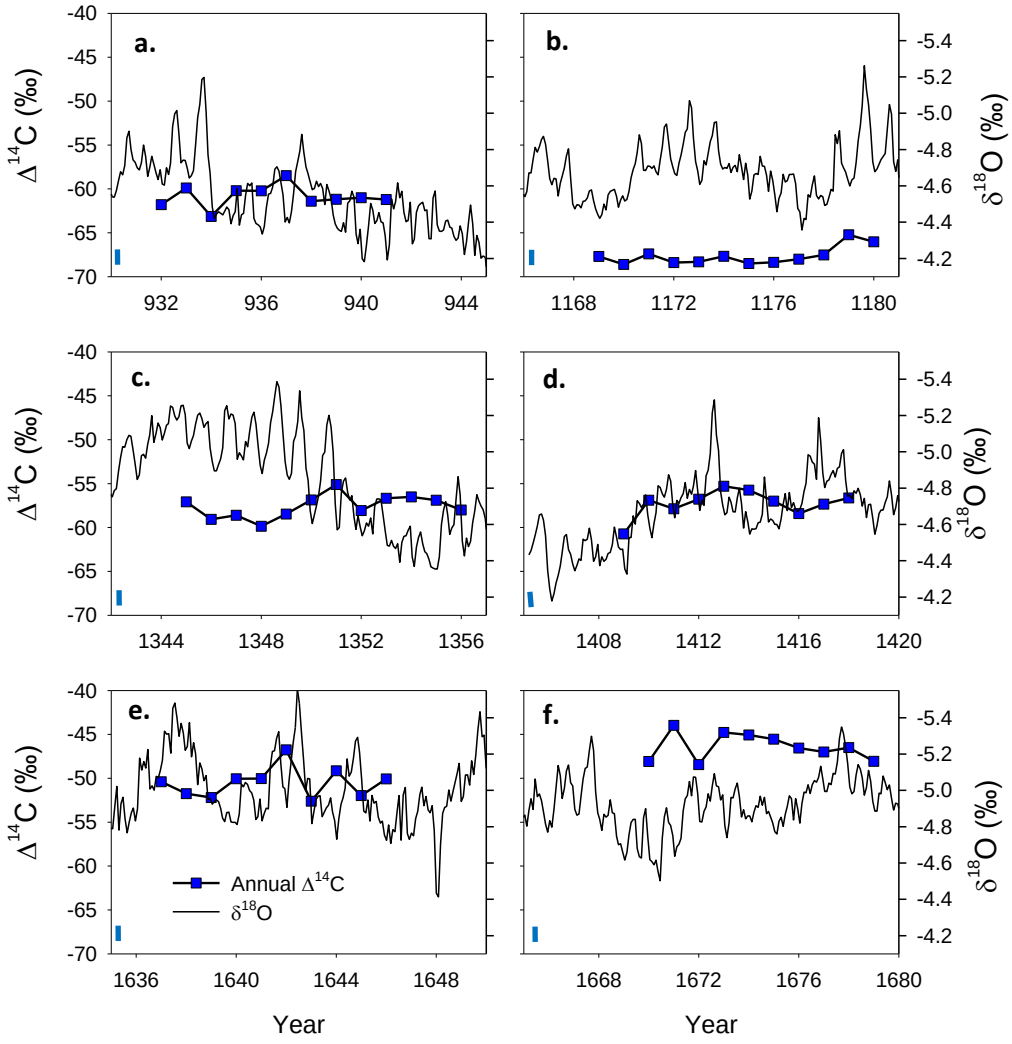

Figure 3.3: Decadal Coral $\Delta^{14}C$ Variability. The vertical blue line represents the ±1.8‰ (1σ) analytical error. a) NB12, b)SB17, c) SB7, d) SB5, e)SB3B, f) SB13. Y-axes for $\delta^{18}O$ and $\Delta^{14}C$ are identical in all plots.

3.3 Centennial ^{14}C Variability

The largest signal in the Line Island coral ^{14}C reconstructions occurs on a centennial timescale, with relatively depleted values during the MCA and relatively

enriched values during the LIA. In comparison to modern pre-bomb ^{14}C values of -54.6‰ (±1.63, N=24) at Palmyra, the 10th and 12th centuries are associated with the most depleted radiocarbon values of the millennium, -60.5‰ (±1.53, N=24) and -67.6‰ (±1.03, N=13), respectively (Figure 3.4). 13th century coral radiocarbon values are also significantly depleted (-60.9‰ ± 4.29, N=22). It is important to note that the 13th century coral contains appreciable secondary aragonite (see Section 3.5), which means that the -61 ^{14}C values measured in this coral represent an upper limit on seawater radiocarbon during this time, which could have been significantly more depleted. Values during the LIA are enriched with respect to the MCA and early 20th century, ranging from -50.3‰ (±1.58, N=25) in the mid-17th century to -46.4‰ (±1.54, N=11) in the late 17th century (Figure 3.4) (Table 3.1). 16th century Christmas coral $\Delta^{14}C$ values are the most enriched of the entire record (-44.6 ± 1.75, N=7). $\Delta^{14}C$ values in the 14th and 15th centuries (-57.6 ± 1.32‰, N=13, -56.8 ± 1.65‰, N=30, respectively) are similar to early 20th century $\Delta^{14}C$ values.

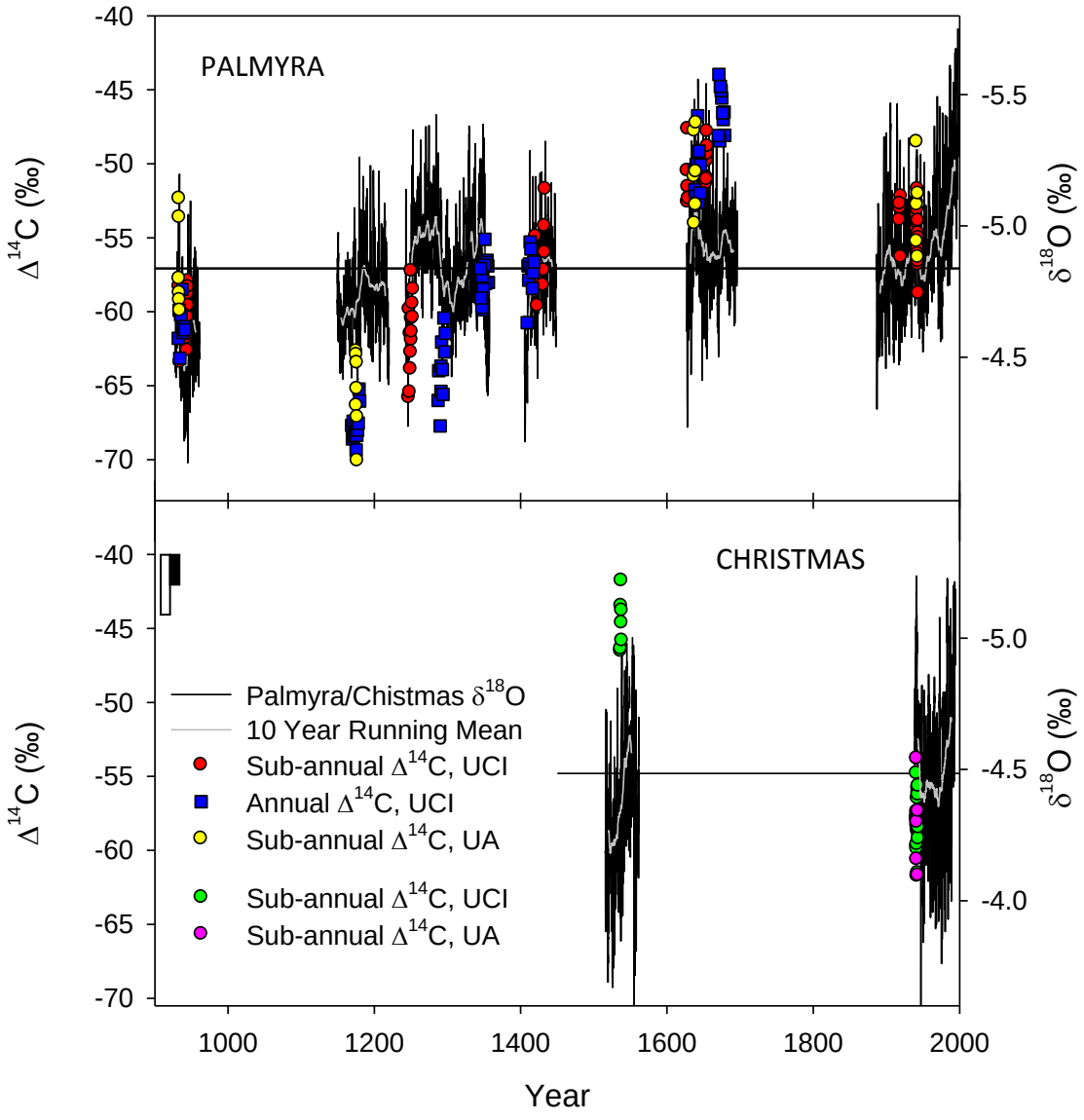

Figure 3.4: Summary of modern and fossil coral $\delta^{18}O$ and $\Delta^{14}C$ data. The thick, black vertical bar represents the ±1.8‰ UCI AMS error; the vertical white bar represents the ±4.0‰ UA AMS error. The horizontal black lines indicate both the average $\delta^{18}O$ and $\Delta^{14}C$ values of the entire records.

Table 3.1: Coral U/Th ages, average $\Delta^{14}C$ and average $\delta^{18}O$

Sample	Island	U/Th Dates*	AMS	$\Delta^{14}C$, ‰	$\delta^{18}O$,‰
NB12	P	928-961 (± 10 yr)	UCI	-60.5 ± 1.53 (N=24)	-4.58
			UA	-56.9 ± 3.16 (N=6)	
L17	P	1149-1220 (± 10 yr)	UCI	-67.6 ± 1.03 (N=13)	-4.73
			UA	-65.4 ± 2.68 (N=7)	
A27	P	1248-1319 (± 5 yr)	UCI	-60.9 ± 4.29 (N=22)	-4.86
SB7	P	1326-1357 (± 5 yr)	UCI	-57.6 ± 1.32 (N=13)	-4.83
SB5	P	1405-1448 (± 5 yr)	UCI	-56.8 ± 1.65 (N=30)	-4.78
M2****	C	1515-1561(± 5 yr)	UCI	- 44.6 ± 1.75 (N=7)	-4.36
SB3B	P	1627-1658 (± 5 yr)	UCI	-50.3 ± 1.58 (N=25)	-4.85
			UA	-50.5 ± 2.68 (N=6)	
SB13	P	1653-1695 (± 5 yr)	UCI	-46.4±1.54 (N=11)	-4.90
Modern	P	1886-1998 (± 2 months)**	UCI	-53.6 ±1.62 (N=5)	-4.91
modern	P	1938-1944 (± 2 months)	UCI	-54.8 ±1.58 (N=24)	-4.91
			UA	-53.0 ± 3.05 (N=5)	
PP7-3	C	1938-1993 (± 2 months)***	UCI	-58.1 ±1.73 (N=24)	-4.51
			UA	-54.6 ± 1.95 (N=6)	

P = Palmyra Island, C = Christmas Island. Analytical error of UCI-KCCAMS radiocarbon measurements is ±1.8‰ (1σ). Analytical error for UA-AMS radiocarbon measurement is ±4.0‰. Error for $\delta^{18}O$ is ±0.05‰ (1σ).
*U/Th dates and uncertainties reported in Cobb et al., [2003a].
** Palmyra modern coral age model reported in Cobb et al., [2001].
***Christmas modern coral age model reported in Evans et al., [1999].
****Unpublished U/Th age and $\delta^{18}O$ data, to be reported in Cobb et al., in prep.

3.4 Mixed Layer Model Constraints on the Sources of coral ^{14}C Variability

The Palmyra mixed layer model suggests that atmospheric ^{14}C variations explain most, though not all, of the centennial-scale ^{14}C variability recorded in the Palmyra and

Christmas fossil corals (Figure 3.5). Our results suggest that atmospheric ^{14}C variability explains average coral ^{14}C values for the 10^{th}, 15^{th}, 17^{th}, and 20^{th} centuries, but that coral ^{14}C values during the 12^{th}, 13^{th}, and 16^{th} centuries likely reflect change in ocean circulation. Potential sources of seawater ^{14}C variability at Palmyra include changes in the rate of equatorial upwelling and/or significant changes in the ^{14}C content of higher-latitude source waters advected to the equatorial thermocline (either from the northern or southern hemisphere). Using the inverse version of the Palmyra mixed layer model, I calculate that a two-fold increase in upwelling would explain the anomalously depleted 12^{th} century Palmyra coral ^{14}C values, while a two-fold decrease in upwelling would explain the anomalously enriched 16^{th} century Christmas coral ^{14}C values. Our simple box model is clearly incapable of constraining the influence of potential changes in source water ^{14}C content or circulation that could account for the observed centennial-scale coral ^{14}C variability.

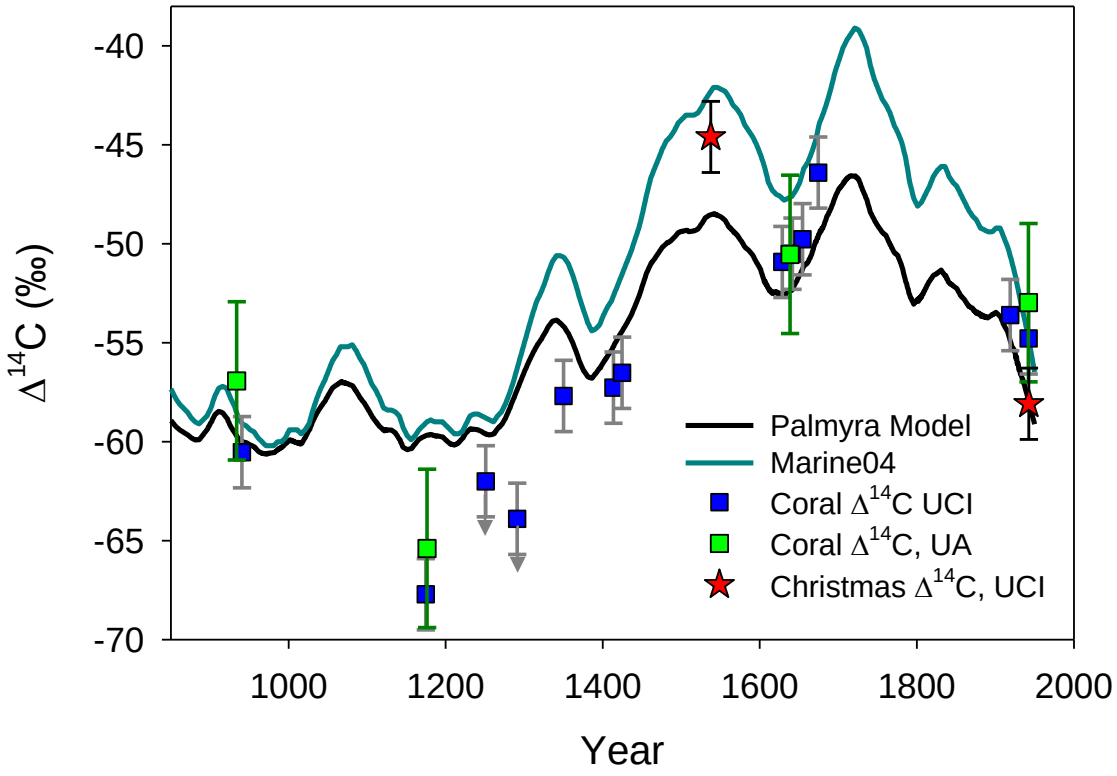

Figure 3.5 –Comparison of Mixed Layer Model of Palmyra ^{14}C with coral ^{14}C. Model output (black curve) is plotted with average coral radiocarbon values from each time horizon and Marine04 (blue curve) [*Hughen et al*., 2004]. Error bars represent the analytical error, ±1.8‰ UCI, ±4.0‰ University of Arizona (UA).

3.5 Diagenesis Screening

The majority of the Palmyra coral collection was previously examined for diagenesis using XRD and thin-sections [*Cobb et al.,* 2002], but these techniques cannot resolve subtle diagenesis that could compromise coral-based seawater ^{14}C reconstructions. A pristine coral skeleton has a smooth, solid surface with easily identifiable dissepiments, and unfilled pore spaces (Figure 3.6). Secondary aragonite

deposition in corals occurs as tiny needles protruding from the original skeleton into open pore spaces, and is commonly associated with submarine diagenesis [*Enmar et al.*, 2001; *Hendy et al.*, 2007] (Figure 3.7a). The SEM photos suggest that the modern Palmyra coral, 10th century coral (NB12), 12th century coral (L17),14th century coral (SB7), and 15th century coral (SB5), all retain relatively pristine coral skeletons lacking obvious signs of secondary aragonite deposition and/or major dissolution (Figure 3.6).

As diagenesis would cause an enrichment in coral ^{14}C values, I used SEM photos to determine whether diagenesis could have caused the ^{14}C enrichments observed in the 16th and 17th centuries fossil corals. Indeed, SEM photos of Palmyra coral SB3B, dated to the mid-17th century, revealed areas in the oldest portion of the core that were covered in small secondary aragonite needles (Figure 3.7a). Radiocarbon values from this horizon average -50.9‰ (±2.01, N=6). However, samples taken from younger bands in the same coral lack any evidence of diagenesis, yet are similarly enriched in ^{14}C (averaging -49.8‰, ±1.09, N=12) (Figure 3.7b). Furthermore, the late 17th century coral (SB13) is even more ^{14}C-enriched than SB3B, yet shows no signs of diagenesis (Figure 3.7d). SEM photos also rule out the influence of diagenesis in causing the very enriched ^{14}C values measured in the 16th century Christmas fossil coral M2 (-44.6‰, ±1.75, N=7). Taken together, these lines of evidence suggest that the minor diagenesis observed in some LIA fossil corals did not affect the ^{14}C content of these corals.

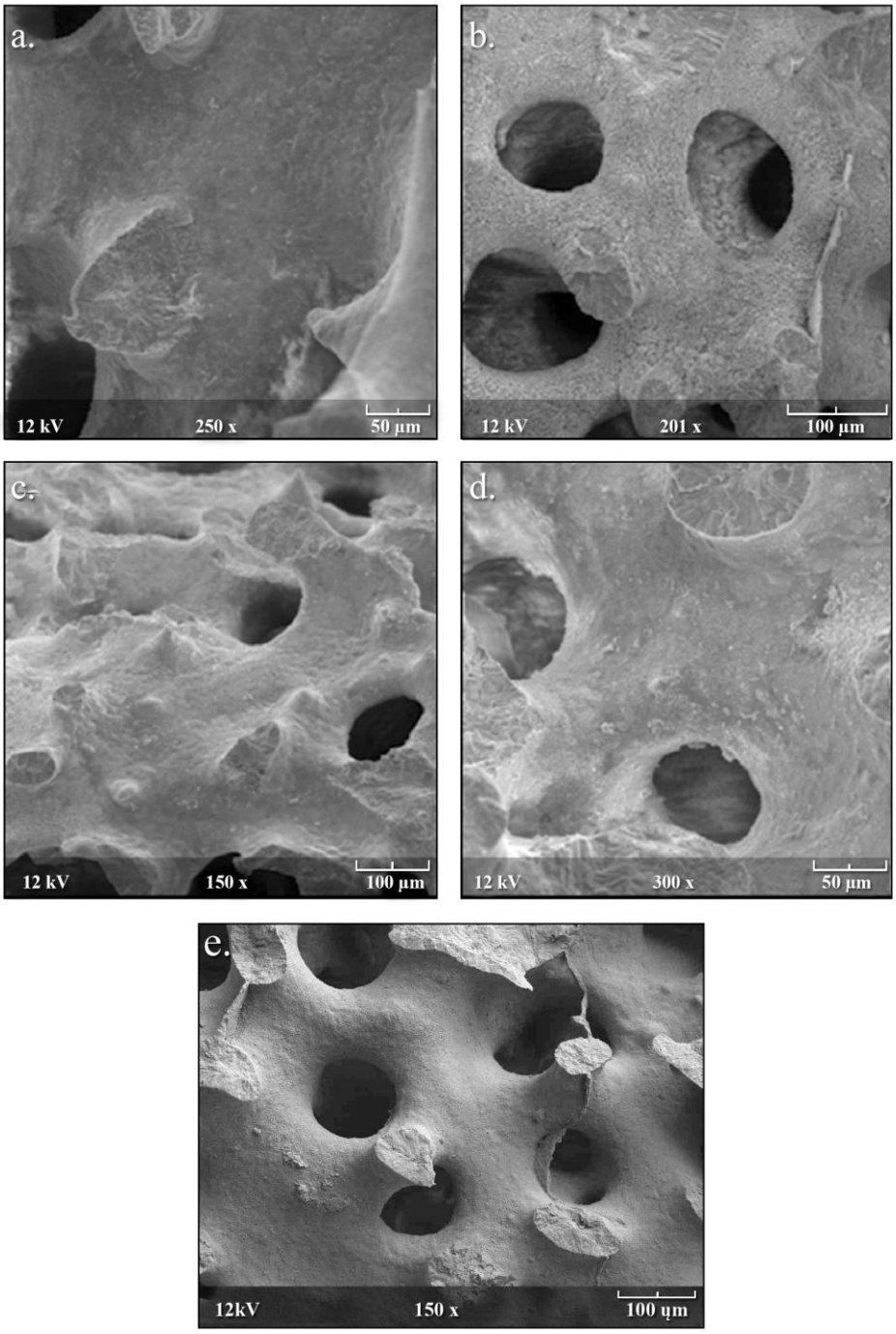

Figure 3.6 – Pristine Coral SEM photos: Examples of pristine modern and fossil corals, a) Palmyra Modern, b) NB12 (~930AD), c) SB5 (~1430AD), d) SB13 (~1760AD). e) Christmas Coral M2 (~1550AD). L17 and SB7 not shown.

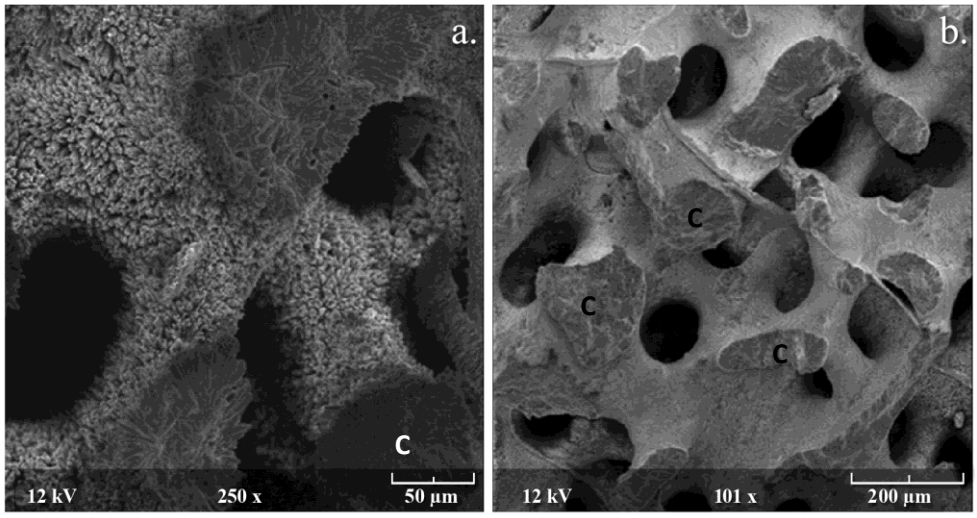

Figure 3.7 – SEM photos of Coral SB3B a) from the base of the core, where many secondary aragonite needles cover the original surface of the coral skeleton, b) midway up the core, where the skeleton is smooth and retains the original skeletal structure. Radiocarbon values from the two sections are nearly identical regardless of the small diagenetic alterations down core. C marks location of chipped surfaces.

Moderate to severe diagenesis in a 13th century fossil coral (A27) was revealed by ^{14}C values of up to -21‰, far outside the range of seawater $\Delta^{14}C$ values in the surface ocean. Such high coral ^{14}C values can only be explained by the addition of relatively young secondary carbonates to the original coral skeleton. In fact, mass balance calculations suggest that portions of this coral must be contaminated with as much as 50% of early 20th century carbonates to obtain values approaching -21‰. Of course, if the contaminating material contains bomb radiocarbon, far less material would be required to cause the observed enrichments. SEM photos of A27 revealed severe dissolution in parts of the coral (Figure 3.9a) in conjunction with smooth, platy crystals that cover large sections of the coral skeleton (Figure 3.9b,c,d). X-ray diffraction (XRD)

analysis of the most altered portion of A27 revealed traces of calcite, as sometimes observed in much older, heavily altered fossil corals [*McGregor et al.,* 2003]. The ^{14}C values measured on more pristine portions of this coral (Figure 3.8) are interpreted as upper limits on seawater ^{14}C during this time, as diagenesis may be masking more significant ^{14}C depletions during this time.

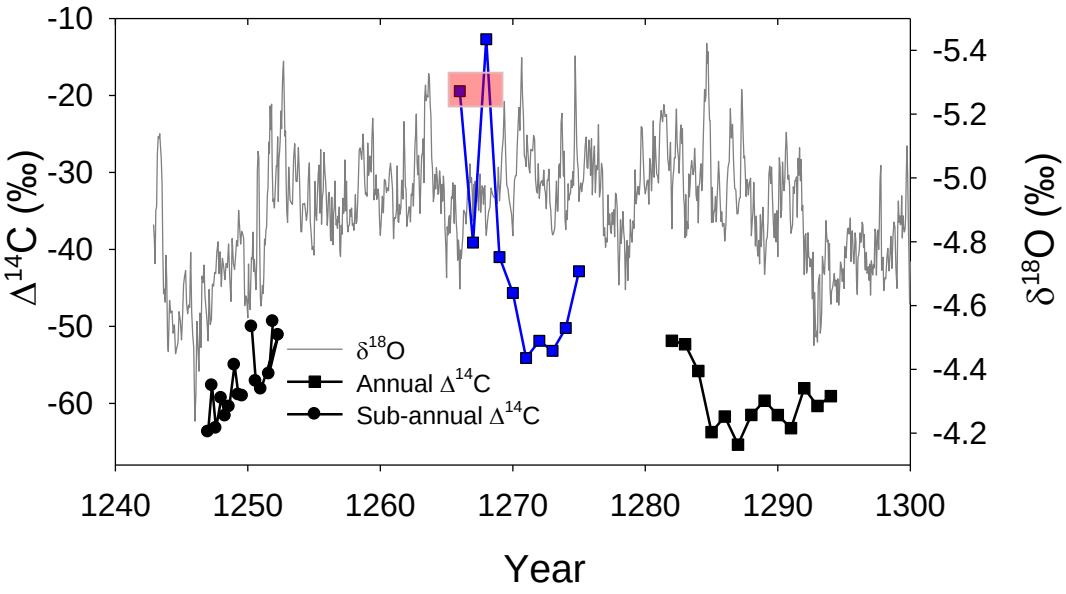

Figure 3.8: Signs of diagenesis in 13th Century Coral ^{14}C Variability. The pink box encloses sample horizons which are associated with significant diagenetic alteration, specifically dissolution and the addition of secondary calcite, as evidenced by SEM photos (Figure 3.9) and XRD analysis. Black symbols represent ^{14}C measurements from more pristine portions of the coral, and represent upper limits on seawater ^{14}C during these times.

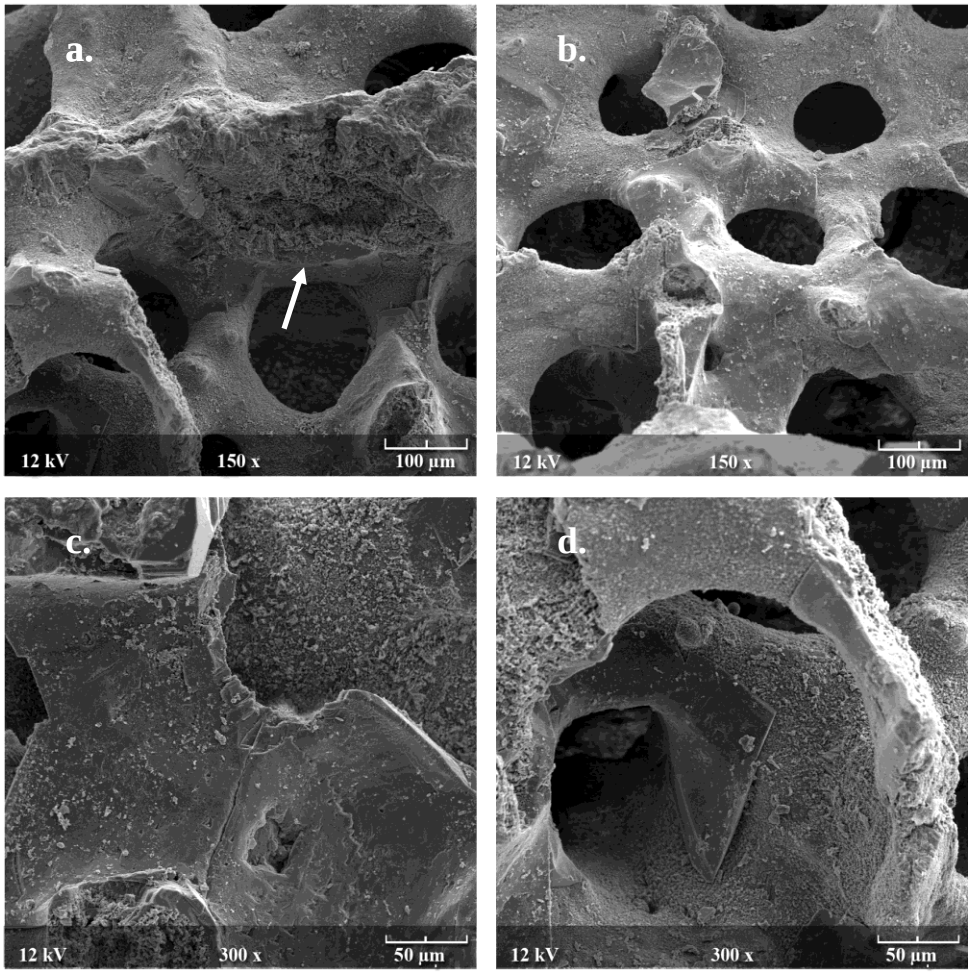

Figure 3.9 – SEM photos of 13th century coral diagenesis. a) section of coral skeleton with massive dissolution, indicated by white arrow, b) solid, platy crystals covering large sections of the original coral skeleton, c),d) enlargement of platy crystals. (See Figure 3.8 for location of SEM photos with respect to isotopic values at that location.) Further testing by XRD has identified these plates as calcite.

4. DISCUSSION

4.1 Interannual ^{14}C variability in the central tropical Pacific

Palmyra and Christmas coral ^{14}C is unchanged throughout multiple large ENSO cycles over the last millennium, including the very large 1941-43 ENSO cycle. The lack of interannual ^{14}C variability indicates that the surface ocean in the central tropical Pacific is relatively well-mixed with respect to radiocarbon, at least to the depth of wind-driven upwelling. Our results are supported by results from Toggweiler [1995], who used a model of nitrate and carbon concentrations in the surface ocean to demonstrate that the NECC and SEC are not distinguishable in the central tropical Pacific on interannual timescales due to the effective mixing of surface waters in this region, both horizontally and vertically. Indeed, for many geochemical tracers, such as radiocarbon, the zonal structures of the NECC and the SEC are clear only in multi-year averages. Toggweiler [1991] finds that at this particular site in the CTP, seawater ^{14}C is well-mixed to depths of 150m, roughly equivalent to the depth of upwelling. If this is correct, then changes in interannual upwelling and/or horizontal advection in the vicinity of Palmyra and Christmas Islands would not be expected to significantly change seawater radiocarbon concentrations at these sites. It is important to note that heat is exchanged much more rapidly across the air-sea interface than carbon dioxide (1-2 months versus ~10 years for isotopic equilibration), meaning that water masses of different heat contents can possess similar ^{14}C concentrations. Therefore, ENSO-related upwelling events are associated with changes in SST but not with changes in seawater ^{14}C.

The lack of interannual ^{14}C signal at Palmyra is supported by a coral ^{14}C reconstruction from nearby Fanning Island (4°N, 154°W), which shows little to no interannual ^{14}C variations [*Grotolli, 2003*]. Indeed, WOCE data indicate that in the post-bomb era, the low radiocarbon upwelling tongue evident in the eastern equatorial Pacific is effectively mixed away in the central tropical Pacific [*Key et al.*, 2004].

4.2 Decadal to Centennial ^{14}C Variability in the central tropical Pacific

Large decadal signals in coral $\delta^{18}O$ data are not associated with significant coral ^{14}C variability, indicating a decoupling between surface climate and seawater ^{14}C on decadal timescales. This is somewhat surprising, and cannot be explained by different equilibration times of ocean heat versus ^{14}C, as invoked above to explain the lack of interannual ^{14}C variability. One possibility is that surface climate signals and basin-scale circulation reorganizations are lagged by as much as a decade. In other words, a climate signal that originates at the equator might influence higher-latitude climate fairly quickly, but that it might take many years for the changes in high-latitude climate and circulation to make their way into the equatorial thermocline. Such a mechanism has previously been proposed to explain Pacific decadal-scale climate variability (e.g. Gu and Philander, 1997).

Equatorial Pacific seawater ^{14}C concentrations are particularly sensitive to changes in the contribution of relatively ^{14}C-depleted Sub-Antarctic Mode Waters (SAMW) to the equatorial undercurrent. Rodgers [2003] finds that up to 70% of the water reaching the equatorial mixed layer is from the Southern Hemisphere, where

surface radiocarbon values can be as low as -100‰ [*Matsumota and Key*, 2004]. Waters from the Northern Hemisphere are not nearly as depleted (-48‰) [*Druffel et al*., 1993]). Rodgers [2003] found that the fastest transit time for waters subducted from the SAMW to reach the EUC is 28 years, potentially explaining why surface climate changes (as recorded in coral $\delta^{18}O$) and seawater ^{14}C changes (as recorded by coral ^{14}C) in the tropical Pacific could be offset by several decades, and potentially mixed away in the course of transit.

A comparison of the centennial-scale coral $\delta^{18}O$ and ^{14}C records reveals a poor correlation between reconstructed surface climate and paleo-circulation. For example, large $\Delta^{14}C$ anomalies during the 12th and 16th centuries are not associated with significant coral $\delta^{18}O$ anomalies, as expected if upwelling variations were responsible for the ^{14}C depletions and enrichments observed during these periods, respectively. In order to match the 12th and 16th century coral ^{14}C values to the mixed layer model estimates for these periods, the absolute ages of the fossil coral would have to shift by 50-70 years. Conservative estimates of fossil coral U/Th dating errors are ±5 years [*Cobb et al*., 2003a], so dating errors cannot be responsible for the 12th or 16th century model-data mismatch. The decoupling of $\delta^{18}O$ and ^{14}C cannot be explained by alterations to the coral skeleton, as both the 12th and 16th century corals are free of diagenesis. Given the absence of coral $\delta^{18}O$ anomalies on these timescales, we infer that changes in high-latitude source water ^{14}C contributions caused the observed coral ^{14}C anomalies rather than changes in equatorial Pacific upwelling. Relatively small changes in either the ^{14}C of SAMW waters or their relative contribution to the equatorial undercurrent could have caused the ~10‰ departures from the atmospheric mixed layer model curve. In this case,

we infer a ^{14}C depletion in SAMW waters (or an increase of SAMW contributions to the EUC) during the 12th century, vice versa during the 16th century. Ultimately, the relationship between low-frequency equatorial climate and high-latitude circulation could be tested with ^{14}C-equipped, coupled ocean-atmosphere climate models that can be run for multiple centuries.

4.3 Diagenesis Screening

As discussed previously, the addition of calcite or secondary aragonite to the original coral skeleton introduces younger, relatively ^{14}C-enriched carbonate to the coral skeleton. Diagenetic alterations to Palmyra coral SB3B include secondary aragonite needles on the lower section of the core. The observed diagenesis does not appear to have had an effect on the ^{14}C values presented in this study. There are two possible explanations for this observation. First, it is difficult to generate large $\Delta^{14}C$ anomalies over a period that is short relative to the half-life of radiocarbon. For example, it would require a 10% addition of modern pre-bomb material to raise 17th century $\Delta^{14}C$ by 4‰. Second, it is possible that the alteration occurred immediately after the coral skeleton was formed, before it was deposited onto the beach at Palmyra. In this case, the secondary carbonate would have no measureable effect on coral $\Delta^{14}C$. Indeed, Cohen and Hart [2004] find that secondary aragonite precipitation did not affect the fidelity of their coral radiocarbon ages, concluding that the diagenesis must have occurred shortly after skeletal formation. Although many tracers can be altered by secondary aragonite precipitation or

dissolution (i.e. Hendy et al., 2007), we conclude that the radiocarbon concentrations of young (<1000 yrs old), relatively pristine fossil coral is much less effected due to ^{14}C's long half-life.

In the case of the 13th century fossil coral; which had experienced significant diagenesis (both dissolution and secondary calcite precipitation), coral ^{14}C values were significantly enriched. Previous work indicates that secondary calcite should also cause significant enrichments in coral $\delta^{18}O$ [*Enmar et al*., 2001; *Müller et al*., 2001; *McGregor et al*., 2003]. However, in our case the <5% contribution of secondary calcite should not impact bulk coral $\delta^{18}O$, whereas extremely enriched coral ^{14}C values indicate a high sensitivity to this material (which must be very young, if not post-bomb, in its ^{14}C composition).

We conclude that the accuracy of modern or fossil coral-based seawater ^{14}C reconstructions depends on careful diagenetic screening, ideally with SEM photos. As a screening tool, SEM is far preferable to thin sections, as the small needles of secondary aragonite observed in SEM photos of SB3B were not observed in thin section.

5. CONCLUSIONS

Despite large variations in interannual to decadal surface climate inferred from coral $\delta^{18}O$, we find no accompanying changes in coral ^{14}C, suggesting a decoupling between surface climate and ^{14}C. Such decoupling may stem from the long air-sea equilibration time of ^{14}C versus heat (in the case of interannual variations) and/or changes in the ^{14}C content of extratropical source waters that lead or lag changes in tropical Pacific surface climate (in the case of decadal variations). A centennial-scale increase in coral radiocarbon from the MCA to the LIA is largely explained by centennial-scale changes in atmospheric ^{14}C. However, 12^{th} (16^{th}) century coral $\Delta^{14}C$ data are more depleted (enriched) than mixed layer model estimates, consistent with a two-fold increase (decrease) in upwelling during this time and/or a decrease (increase) in the ^{14}C content of equatorial source waters, requiring further study with ^{14}C-equipped coupled climate models. Minor dissolution and addition of secondary aragonite, as observed with SEM photos, has little effect on the accuracy of our coral-based seawater ^{14}C reconstructions. Moderate to severe diagenesis (marked by extensive dissolution and the addition of secondary aragonite) is associated with significantly high ^{14}C diagenesis-related artifacts.

6. REFERENCES

Allan, R., J. Lindsay, and D. Parker (1996), *El Niño Southern Oscillation and Climatic Variability*, CSIRO, Australia.

Allison, N., A.A. Finch, J.M. Webster, and D.A. Clague (2007) Palaeoenvironmental records from fossil corals: The effects of submarine diagensis on temperature and climate estimates, *Geochimica et Cosmochimica Acta*, 71, 4693-4703.

Bar-Matthews, M., G.J. Wasserburg, and J.H. Chen (1993), Diagenesis of fossil coral skeletons: Correlation between trace elements, textures, and ^{234}U / ^{238}U, *Geochimica et Cosmochimica Acta*, 57, 257-276.

Bjerknes, J., (1969) Atmospheric teleconnections from the equatorial Pacific, *Monthly Weather Review, 97***,** 163-172.

Brown, T, G.W. Farwell, P.M. Grootes, F.H. Schmidt, and M. Stuvier (1993), Intra-annual variability of the radiocarbon of corals from the Galapagos Islands, Radiocarbon, 35, 245-251.

Bryden, H.L., and E.C. Brady (1985), Diagnostic Model of Three-Dimensional Circulation in the Upper Equatorial Pacific Ocean, *Journal of Physical Oceanography*, 15, 1255-1273.

Burr, G.S., R.L. Edwards, D.J. Donahue, E.R.M. Druffel, and F.W. Taylor (1992), Mass Spectrometric ^{14}C and U-Th measurements in coral, *Radiocarbon, 34*(3), 611-618.

Burr, G.S., J.W. Beck, F.W Taylor, J. Recy, R.L. Edwards, G. Cabioch, T. Correge, D. J. Donahue, and J. M. O'Malley (1998) A high resolution radiocarbon calibration between 11,700 and 12,400 calendar years BP derived from ^{230}Th ages of corals from Espiritu Santo Island, Vanuatu, *Radiocarbon*, 40(3), 1093-1105.

Castellaro, C., B. Savary, A. Ribaud-Laurenti, B. Hamelin, L. Montaggioni, A. Juillet-Leclerc, and J. Recy (1999), Influence of marine diagenesis on geochemical records of $\delta^{18}O$, Sr/Ca and U/Ca in Porites skeleton, paper presented at Paleoceanology of Reefs and Carbonate Platforms: Miocene to Modern, ASF, Aix-en-Provence, France.

Chiu, T., R. Fairbanks, R. Mortlock, and A. L. Bloom (2005), Extending the radiocarbon calibration beyond 26000 years before present using fossil corals, *Quaternary Science Reviews*, 24, 1797-1808.

Cobb, K. M., D. E. Hunter, and C. D. Charles (2001), A central tropical Pacific coral demonstrates Pacific, Indian, and Atlantic decadal climate connections, *Geophysical Research Letters*, 28(11), 2209-2212.

Cobb, K.M. (2002), Coral records of the El Niño-Southern Oscillation and tropical Pacific climate over the last millennium, University of California, San Diego

Cobb, K.M., C.D. Charles, H. Cheng, M. Kastner, and R.L. Edwards (2003a), U/Th-dating living and young fossil corals from the central tropical Pacific, *Earth and Planetary Science Letters, 210*, 91-103.

Cobb. K.M., C.D. Charles, R.L Edwards, H. Cheng, and M. Kastner (2003b), El Niño-Southern Oscillation and tropical Pacific climate during the last millennium, *Nature*, 424**,** 271-276.

Cohen A.L. and S.R. Hart (2004), Deglacial sea surface temperatures of the western tropical Pacific: A new look at old coral, *Paleoceanography*, 19, PA4031

D'Arrigo, R., R. Wilson, J. Palmer, P. Krusic, A. Curtis, J. Sakulich, S. Bijaksana, S. Zulaikah, L. O. Ngkoimani, and A. Tudhope (2006), The reconstructed Indonesian warm pool sea surface temperature from tree rings and corals: Linkages to Asian monsoon drought and El Niño-Southern Oscillation, *Paleoceanography*, 21(3), PA3005, doi:10.1029/2005PA001256.

Druffel, E. R.M., (1981) Radiocarbon in annual coral rings from the eastern tropical Pacific Ocean, *Geophysical Research Letters, 8*, 59-62.

Druffel, E.R.M., (1987) Bomb radiocarbon in the Pacific: Annual and seasonal timescale variations, *Journal of Marine Chemistry, 45*, 667-698.

Druffel, E.R.M and S. Griffin (1993), Large variations of surface ocean radiocarbon: Evidence of circulation changes in the southwestern Pacific, *Journal of Geophysical Research*, 98(C11), 20249-20260.

Druffel, E. R. M., S. Griffin, A. Witter, E. Nelson, J. Southon, M. Kashgarian and J. Vogel (1995), *Gerardia*: Bristlecone pine of the deep-sea?, *Geochimica et Cosmochimica Acta***,** 59 (23), 5031-5036.

Druffel, E.R.M., (1997), Geochemistry of Corals: Proxies of ocean chemistry, past ocean circulation, and climate, Proceeding of the National Academy of Science.

Druffel, E.R.M., S. Griffin, M. Kashgaria, J. Southon, D.P. Schrag, (2001) Changes of subtropical North Pacific radiocarbon and correlation with climate variability, *Radiocarbon, 43*, 15-25.

Druffel, E.R.M. (2002) Radiocarbon in Corals: Records of the Carbon Cycle, Surface Circulation and Climate, *Oceanography, 15***,** 122-127.

Druffel, E.R.M, S. Griffin, Jeomshik Hwang, Tomoko Komada, Steven R. Beaupre, Kevin C. Druffel-Rodriguez, Guaciara M. Santos and John Southon (2004), Variability of radiocarbon during the 1760s in monthly corals from the Galapagos Islands, *Radiocarbon, 46(2*), 627-632.

Druffel, E.R.M., S.Griffin, S.R. Beaupre, R.B. Dunbar (2007), Oceanic climate and circulation changes during the past four centuries from radiocarbon in corals, *Geophysical Research Letters*, 34, L096901.

Druffel, E.R.M., and T.W. Linick (1978), Radiocarbon in annual coral rings of Florida, *Geophysical Research Letters*, 5(11), 913-917.

Druffel, E.R.M., and H.E. Suess (1983), On the radiocarbon record in banded corals: exchange parameters and net transport of $^{14}CO_2$ between atmosphere and surface ocean. *Journal of Geophysical Research*, 88, 1271–1280.

Dunbar, R. G., and J. E. Cole (1999), Annual records of tropical systems (ARTS), *PAGES Workshop Report Series*, 99(1), PAGES, BERN Switzerland, 72.

Enmar, R., M. Stein, M. Bar-Matthews, E. Sass, A. Katz, and B. Lazar (2000), Diagenesis in live corals from the Gulf of Aqaba. I. The effect on paleo-oceanography tracers, Geochimica et Cosmochimica Acta, 64 (18), 3123–3132.

Evans, M. N., R. G. Fairbanks, and J. L. Rubenstone (1999), The thermal oceanographic signal of ENSO reconstructed from a Kiritimati Island coral, *Journal of Geophysical Research*, 104, 13409-13421.

Evans, M.N, M.A. Cane, D.P. Schrag. A. Kaplan. B.K. Linsley, R. Villaba, and G.M. Wellington (2001), Support for tropically-driven Pacific decadal variability based on paleoproxy evidence, Geophysical Research Letters, 28(19), 3689-3692.

Fairbanks, R. G., M. N. Evans, J. L. Rubenstone, R. A. Mortlock, K. Broad, M. D. Moore, and C. D. Charles (1997), Evaluating climate indices and their geochemical proxies measured in corals, *Coral Reefs*, 16(Suppl.), S93-S100.

Gagan, M.K., L.K. Ayliffe, J.W. Beck, J.E. Cole, E.R.M. Druffel, R.B. Dunbar and D.P. Schrag, (2002) New Views of Tropical Paleoclimates from Corals, *Quaternary Science Reviews, 19***,** 45-64.

Grumet, N. S, N. J. Abram, J. W. Beck, R. B. Dunbar, M. K. Gagan, T. P. Guilderson, W. S. Hantoro, and B. W. Suwargadi (2004) Coral radiocarbon records of Indian

Ocean water mass mixing and wind-induced upwelling along the coast of Sumatra, Indonesia, *Journal of Geophysical Research,* 109, C05003, doi:10.1029/2003JC002087.

Guilderson, T.P., Schrag, D.P., (1998a), Radiocarbon variability in the western equatorial Pacific inferred from a high-resolution coral record from Nauru Island, *Journal of Geophysical Research,* 103, 24,641–24,650.

Guilderson, T. and Schrag, D., (1998b) Abrupt shift in subsurface temperatures in the tropical Pacific associated with changes in El Nino, *Science, 201*, 240-243.

Gu, D., and S. G. H. Philander (1997), Interdecadal climate fluctuations that depend on exchanges between the tropics and the extratropics, *Science,* 275, 805-807.

Graham, N. E. (1994), Decadal-scale climate variability in the tropical and North Pacific during the 1970s and 1980s: Observations and model results, *Climate Dynamics*, 10, 135-162.

Graham,N.E., (2004) Late Holocene teleconnections between tropical Pacific climate variability and precipitation in the western USA: evidence from proxy records, *The Holocene, 14*(3), 436-447.

Graham, N.E., M.K. Hughes, C.M. Ammann, K.M. Cobb, M.P. Hoerling, D.J. Kennett, J.P. Kennett, B. Rein, L. Stott, P.E. Wigand, T. Xu, (2007) Tropical Pacific –mid-latitude teleconnections in medieval times", *Climate Change, 83,* 241-285.

Grottoli, A.G, S.T. Gille, E.R.M. Druffel, R.B. Dunbar, (2003), Decadal timescale shift in the ^{14}C record of a central equatorial Pacific coral, *Radiocarbon,* 45(1), 91-99.

Hare, S.R, and N.J. Mantua (2000), Empirical evidence for North Pacific regime shifts in 1977 and 1989, *Progress in Oceanography,* 47 (2-4), 103-145.

Hendy, E.J., M.K. Gagan, J.M. Lough, M. McColluch and P.B. deMenocal (2007), Impact of skeletal dissolution and secondary aragonite on trace element and isotopic climate proxies in Porites corals, *Paleoceanography,* 22, PA4101

Hughen, K.A., M.G.L. Baille, E. Bard, J.W. Beck, C.J.H. Bertrand, P.G. Blackwell, C.E. Buck, G.S. Burr, K.B. Cutler, P.E. Damon, R.L. Edwards, R.G. Fairbanks, M. Friedrich, T.P. Guilderson, B. Kromer, G. McCormac, S. Manning, C.B. Ramsey, P.J. Reimer, R.W. Reimer, S. Remmele, J.R. Southon, M. Stuiver, S. Talamo, F.E. Taylor, J. ver der Plicht, C.E. Weyhenmeyer (2004), Marine04 Marine Radiocarbon Age Calibration, 0-26 CAL KYR BP, *Radiocarbon*, 46(3), 1059-1086.

Intergovenmental Panel on Climate Change (IPCC) (2007), Working Group I: The Physical Basis of Climate Change, Fourth Assessment Report (AR4)

Johnson, G., M. McPhaden, G. Rowe, and K. McTaggart (2000), Upper equatorial Pacific Ocean current and salinity variability during the 1996–1998 El Niño–La Niña cycle, *Journal of Geophysical Research*, 105(C1), 1037-1053.

Kessler, B.A and W.S. Taft (1987) Variations in zonal currents in the central tropical Pacific during 1970 to 1987: Sea level and dynamic height measurements, *Journal of Geophysical Research*, 96, Issue C7, 12599-12618.

Key, R.M., P.D. Quay, G.A. Jones, A.P. McNichol, K.F. Von Reden, and R.J. Schneider (1996) WOCE AMS Radiocarbon I: Pacific Ocean Results (P6, P16, P17), *Radiocarbon, 38*(3), 425-518.

Key, R.M., P.D. Quay, P. Schlosser, A.P. McNichol, K.F. von redden, R.J. Schneider, K.L. Elder, M. Stuiver, H.G. Ostlund (2002), WOCE Radiocarbon IV: Pacific Ocean results; P10, P13N, P14C, P18, P19 & S4P, *Radiocarbon*, 44(1), 239-392.

Konishi, K., T. Tanaka, and M. Sakanoue (1981), Secular variations of radiocarbon concentrations in seawater: sclerochronological approach, *Proceedings of the Fourth International Coral Reef Symposium*, 1:181-5.

Mantua, N. J., S. R. Hare, Y. Zhang, J. M. Wallace, and R. C. Francis (1997), A Pacific interdecadal climate oscillation with impacts on salmon production, *Bulletin of the American Meteorological Society*, 78(6), 1069-1079.

Marzaioli, F, G. Borriello, I. Passariello, C. Lubritto, N. De Cesare, A. D'Onofrio, and F. Terrasi (2008), Zinc reduction as an alternative method for AMS radiocarbon dating: Process optimization at CIRCE, *Radiocarbon*, 50(1), 1-11.

Matsumoto, K., and R.M. Key (2004), Natural Radiocarbon Distribution in the Deep Ocean, *Global Environmental Change in the Ocean and on Land*, 45–58.

McGregor, H. and M.K. Gagan (2003), Diagenesis and geochemistry of *Porites* corals from Papua New Guinea: Implications for paleoclimate reconstruction, Geochimica et Cosmochimica Acta, 67 (12), 2147–2156.

McPhaden, M. J., and D. Zhang (2002), Slowdown of the meridional overturning circulation in the upper Pacific Ocean, *Nature*, 415, 603-608.

Miller, A.J., D.R. Cayan, T.P. Barnett, N.E. Graham, and J.M. Oberhuber (1994) The 1976-77 Climate shift of the Pacific ocean, *Oceanography*, 7(1), 21-26.

Müller, A., M.K. Gagan, M.T. McCulloch (2001) Early marine diagenesis in corals and geochemical consequences for paleoceanographic reconstructions, *Geophysical Research Letters,* 28 (23), 4471-4474.

Nozaki, Y., D.M Rye, K.K Turkian, R.E Dodge, (1978) A 200 year record of carbon-13 and carbon-14 variations in a Bermuda coral, *Geophysical Research Letters, 5* (10), 825-828.

Nydal, R., and K. Loveseth (1983), Tracing Bomb ^{14}C in the Atmosphere, *Journal of Geophysical Research,* 88, 3621-3646.

Ostlund, H.G. and M. Stuvier, (1980) GEOSECS Pacific Radiocarbon, *Radiocarbon, 22*(1), 25-53.

Picaut, J. and R. Tournier, (1991) Monitoring 1979-1985 equatorial Pacific transports with expendable bathythermograph data, *Journal of Geophysical Research, 96,* Supplement, 3263-3277.

Reimer, P., M.G. L. Baillie, E. Bard, A. Bayliss, J.W. Beck, C.J.H. Bertrand, P.G. Blackwell, C.E. Buck, G. S. Burr, K.B. Cutler, Paul E.Damon, R Lawrence Edwards, Richard G Fairbanks, M. Friedrich, T. P. Guilderson, A. G. Hogg, K.A. Hughen, Bernd Kromer, G.McCormac, S. Manning, C. Bronk Ramsey, R. W. Reimer, S. Remmele, J.R. Southon, M. Stuiver, S. Talamo, F. W. Taylor, J. van der Plicht, C. E Weyhenmeyer (2004), IntCal04 terrestrial radiocarbon age calibration, 0 – 26 cal kyr BP, Radiocarbon, 46, 1029–1059.

Reynolds, R. W., and T. M. Smith (2004), Improved global sea surface temperature analyses using optimum interpolation,

Rodgers, K. (2003), Extratropical sources of Equatorial Pacific upwelling in a OGCM, *Geophysical Research Letters, 30*(2), 1084.

Rodgers, K.B., D.P. Schrag, M.A. Cane, and N.H. Naik (2000), The bomb ^{14}C transient in the Pacific Ocean. Journal of Geophysical Research, 105, 8489–8512.

Rodgers K. and Cane (1997), Seasonal variability of sea surface ^{14}C in the equatorial Pacific in an ocean circulation model, *Journal of Geophysical Research*, 102 (C8), 18627-18639.

Rodgers, K.B., O. Aumont, G. Madec, and C. Menkes (2004), Radiocarbon as a thermocline proxy for the eastern equatorial Pacific, *Geophysical Research Letters, **31***, L14314-L14318.

Slota, P.J., A.J.T. Jull, T.W. Linick, and L.J. Toolin (1987), Preparation of small samples for ^{14}C accelerator targets by catalytic reduction of CO, *Radiocarbon*, 29(2), 303-306.

Smith, T.M., R.W. Reynolds, Thomas C. Peterson, and Jay Lawrimore (2007) Improvements to NOAA's Historical Merged Land-Ocean Surface Temperature Analysis (1880-2006), *Journal of Climate*, 20(22), 5473–5496.

Southon, J., G. Santos, K.C. Druffel-Rodrigues, E.R.M. Druffel, S. Trumbore, X. Xu, S. Griffin, S. Ali, and M. Mazon (2004), The Keck Carbon Cycle AMS Laboratory, University of California, Irvine: Initial operation and a background surprise, *Radiocarbon*, 46 (1), 41-49.

Stuiver, M., (1961) Variations in Radiocarbon Concentration and Sunspot activity, Journal of Geophysical Research, 66(1), 273-276.

Stuiver, M., and H.A. Polach, (1977), Discussion reporting of ^{14}C data, *Radiocarbon*, 19(3), 355-363.

Stuiver, M. and Quay, P. (1981), Atmospheric ^{14}C changes resulting from fossil fuel CO_2 release and cosmic ray flux variability. *Earth and Planetary Science Letters* 53: 349-362.

Suess, HE. (1953), Natural radiocarbon and the rate of exchange of carbon dioxide between the atmosphere and the sea, *Proceedings of the Conference on Nuclear Processes in Geological Settings*. Chicago: University of Chicago Press. p 52–60.

Suess, H.E. (1955), Radiocarbon concentration in modern wood. *Science* 122: 415.

Taft B.A., and W.S. Kessler (1991), Variations of zonal currents in the central tropical Pacific during 1970 to 1987: sea level and dynamic height measurements", *Journal of Geophysical Research, 96*, 12599-12618.

Takahashi, T (2004), The Fate of Industrial Carbon Dioxide, *Science*, 305 (5682), 352 – 353. DOI: 10.1126/science.1100602

Toggweiler, J.R., Dixon, and Bryan, K., (1989a) Simulations of Radiocarbon in a coarse resolution World Ocean Model 1: Steady-state pre-bomb distributions, *Journal of Geophysical Research*, 94 (C6), 8217-8242.

Toggweiller, J.R. and K. Dixon, (1991), The Peru upwelling and the ventilation of the South Pacific thermocline, *Journal of Geophysical Research*, *96*, C11, 20467-20497.

Vogel, J.S, J.R. Southon, D.E. Nelson, T.A. Brown, (1984), Performance of catalytically condensed carbon for use in accelerator mass spectrometry, *Nuclear Instruments and Methods in Physics Research, B5*, 289-293.

Weber, J.N. and P.M.J. Woodhead (1972), Temperature dependence of Oxygen-18 concentration in Reef Coral Carbonate, *Journal of Geophysical Research*, 77, 463-473.

Weisberg, R. H., and L. Qiao, (2000), Equatorial upwelling in the central Pacific estimated from moored velocity profilers, *Journal of Physical Oceanography, 30*, 105–124.

Wyrtki, K., and B. Kilonsky (1984), Mean water and current structure during the Hawaii-to-Tahiti Shuttle Experiment, Journal of Physical Oceanography, 14, 242-254.

Zhang, Y., J. M. Wallace, and S. Battisti (1997), ENSO-like interdecadal variability: 1900-93, *Journal of Climate*, 10(5), 1004-1020.